INTERNATIONAL, JOURNAL OF SCIENCE & SOCIETY YABATECH
VOL 7, No 1, JUNE 2021. ISSN: 2276-7924

MICROBIOLOGICAL QUALITY ASSESSMENT OF AFRICAN WALLNUT (*Tetracarpidium conophorum)* OBTAINED FROM SELECTED AREAS OF YABA METROPOLIS, LAGOS NIGERIA

***Balogun,** P. O.[1]**, Coker**, F. C.[1], **Amolegbe**, O. A.[2] and **Balogun**, O. B.[3]

[1,3]Department of Biological Science, Yaba College of Technology, Lagos, Nigeria
[2]Department of Microbiology, University of Lagos, Lagos, Nigeria
[4]Department of Microbiology, Joseph Ayo Babalola University, Ikeji Arakeji, Osun State

Corresponding Author: *peter.balogun@yabatech.edu.ng, 07033691748*

ABSTRACT

African walnut (*Tetracarpidium conophorum*) is a tropical fruit with high nutritional composition and various health benefits. This study investigated the microbial load in raw and cooked African walnuts sold for immediate consumption within Yaba Metropolis Lagos. In this research, a total of fifty six (56) African walnut samples were analysed. The raw samples were purchased from Oyingbo Market, Lagos Nigeria while cooked samples were purchased from five different hawkers within Yaba Metropolis Lagos. Stock solutions of the walnut samples were prepared and microbial isolations were carried out, using pour plate method on Nutrient Agar, Eosin Methylene Blue Agar, Mannitol Salt Agar, *Salmonella Shigella* Agar for bacteria and Potato Dextrose Agar for fungi. Morphologically, the results showed that bacterial isolates were shinny, soft, opaque and mostly regular in shape. Within the seven days, the microbial load ranged from $0.3x10^4$cfu/ml to $1.1x10^5$cfu/ml; $0.6x10^5$cfu/ml to $1.1x10^5$cfu/ml and $0.6x10^5$cfu/ml to $1.8x10^5$cfu/ml, for raw, cooked and hawked walnut respectively. The biochemical identification revealed more of Gram negative bacteria; *Pseudomonads* spp, *Salmonella* spp, *Citrobacter* spp, *Klebsiella* spp, *Escherichia coli* and *Pseudomonads aeruginosa* than the Gram positive bacteria; *Micrococcus* spp, *Staphylococcus* spp, *Staphylococcus aureus* and *Bacillus* spp. The presence of enteric bacteria was considered an indication of poor hygiene during cooking and handling process. No fungal growth was however observed within the period of evaluation. It was concluded that proper washing with clean water, refrigeration or immediate consumption of African walnuts after cooking will help prevent its spoilage and eliminate cross infection in the consumers.

KEYWORDS: African-walnut, Enteric-bacteria, Infection, Quality, Spoilage.

1.0 INTRODUCTION

African walnut (*Tetracarpidium conophorum*) is a member of the Euphorbiaceae family. It is found in the wet parts of Eastern and Western Nigeria as well as Western Africa in general. It is known in Eastern Nigeria as Ukpa (Igbo), Western Nigeria as "Awusa or Asala" (Yoruba), "Okhue or Okwe" (Edo) (Ayoola *et al*., 2011). *Tetracarpidium conophorum* is a climbing shrub of about 10-20ft long, it is normally planted under an indigenous tree so that can provide strong support for the heavy weight of the climber when fully established on the crown of the tree, and in some cases where they cannot be harvested manually; they are left till full maturation after which the pods fall off and are picked, removed from the rotten pods, washed and sold in the market (Dauda *et al.,* 2020).

Conophor plants are generally cultivated for the nuts which are commonly cooked and consumed as snacks. The walnut shells could be black or brown from the plant. The nut is whitish upon cracking from the shell and there is usually a thin layer in between two halves of the nut when it is divided into two equal parts (Ayoola *et al*., 2011).

Studies have indicated that African walnut is rich in protein, fat and carbohydrate but low in fibre and ash contents. Research has proved nuts to be very good sources of Vitamins A, B1, B2, B6, E, folate, sodium, potassium, manganese, copper, chloride, iron and ascorbic acid. The green hulls or the immature fruits are found as good sources of vitamin C. The nut is a good source of energy as it has about (16.9%) carbohydrate and calories of about 600J. It is also an excellent source of polyunsaturated fatty acids such as alpha-linolenic acid (ALA). The nuts of *Tetracarpidium conophorum* is an excellent source of anti-inflammatory omega-3

– essential fatty acids. In terms of phytonutrients, walnuts contain antioxidants and anti-inflammatory compounds including more than a dozen phenolic acids, and a wide variety of flavinoides. It also contains a very high composition of vitamin E, most especially, gamma-tocophenol (Kanu *et al.*, 2015).

It was reported that hot aqueous extract from *Tetracarpidium conophorum* nut could help to protect rats against castor oil-induced diarrhea; the inhibitory effect was attributed to the presence of some secondary metabolites and which also justified ethno medicinal use **(**Nwachoko and Jack 2015).

The seeds of *Tetracarpidium conophorum* are used in Nigeria to increase sperm counts in men (Obayendo, 2013). Also Nwauzoma and Dappa (2013) reported that *Tetracarpidium conophorum* boiled seeds can also be eaten to improve sperm count in men. It was proved that the extract of *Tetracarpidium conophorum* seed increases the viability and sperm output of male albino rats and this suggests that the seed could be included in the formulation of male fertility drugs (Ikpeme *et al.*, 2014).

However, Dada and Aguda, (2015) reported that the*Tetracarpidium conophorum* seed powder has potential pro-fertility properties in male *Clarias gariepinus* (African sharp tooth catfish) that could be exploited in fish production as a feed additive for the improved reproductive performance of male African catfish. Evaluation of the chloroform extract of the *Tetracarpidium conophorum* fruit shows that a 400 mg/kg dose significantly inhibited inflammation when compared with diclofenac but 200 mg/kg of the extract was pro-inflammatory (Olaniyi *et al*., 2016).

The nuts of *Tetracarpidium conophorum* was said to have the potential to reduce hyperglycaemia; researchers also reported that the nuts increased the haemoglobin level and decreased urine output in the test group when compared with controls and could prevent diabetes associated with renal damage **(**Onwuli *et al*., 2014 and Ogunyinka *et al*., 2015). Another study carried out by Ogbonna *et al*., (2013) indicated a significant reduction in blood glucose level and suggested that the leaf and the root extracts of *Tetracarpidium conophorum* are more potent in lowering blood glucose in alloxan-induced diabetic rats when compared with oral hypoglycemic agents. Similar studies were carried out by Ogbonna *et al*., (2015) on the effect of root and leaf extracts of *Tetracarpidium conophorum* in alloxan-induced diabetic rats and showed a significant increase ($p < 0.01$) of Alanine aminotransferase (ALP), Aspartate aminotransferase (AST) and Alkaline phosphatate (ALT), which indicated that the leaf and root extracts possess anti-diabetic and hepatoprotective activity. *Pan et al*. (2013) and Zibaeenezhad *et al*. (2017) also established the consumption of walnut to lower risk of type II diabetes among women though it was insignificant to control body mass index.

Without doubt, the nuts of *Tetracarpidium conophorum* have so many health benefits. However, spoilage of these nuts is commonly observed especially when bought from hawkers on high ways or in the street. It is therefore the aim of this research to identify the bacterial and fungi that are present in raw and cooked African walnut sold for immediate consumption in Yaba Metropolis, Lagos Nigeria.

2.0 MATERIALS AND METHODS

2.1 SAMPLE COLLECTION

Raw samples (uncooked walnut) were sourced from Oyingbo Market in Lagos while cooked samples were purchased from five different hawkers around Yaba Metropolis, Lagos and transferred in a Ziploc bags to the laboratory for onwards microbiological analysis. A total of 56 African walnuts were sampled and divided into eight (8) groups; A to H. One (1) sample each from each of the eight groups was taken each day blended and analyzed per day for seven consecutive days**.** Samples were maintained under normal ambient temperature similar to that of hawking environment.

2.2 BIOCHEMICAL IDENTIFICATION OF BACTERIAL ISOLATED FROM RAW AND HAWKED WALNUT SAMPLES

Isolated bacterial were subjected to the following biochemical tests; catalase, oxidase, urease, indole, citrate utilization, coagulase, lactose, glucose, hydrogen sulphide, gas production, motility, mannitol, and spore test respectively**.**

2.3 ISOLATION OF BACTERIAL

From each group, a sample was picked, cracked and weighed (g) using an electronic sensitive balance separately then transferred into a pre-sterilized mechanical blender where sterile water was added in the ratio of 1:9 (walnut in gram: sterile water) before blending; this forms

the stock solution. From this solution, further 10 fold dilutions up to 10^{-3} were prepared. Pour plate method was used in this process for the isolation of bacterial. One (1) ml each of inoculums from dilution factor 10^{-3} was aspirated into the pre-labeled sterile petri dishes and the molten agar media; Nutrient Agar (NA), Eosin Methylene Blue (EMB), Mannitol Salt Agar (MSA), Salmonella Shigella Agar (SSA) were and respectively poured and incubated at 37^{o}C for 24 - 48hrs for the isolation of bacterial

2.4 ISOLATION OF FUNGI

From each of the stock solutions made, pour plate method was used for the isolation of fungi on Potatoes Dextrose Agar (PDA) and incubated at 28^{o}C for 3-5 days.

3.0 RESULTS

Microbiological analysis of the raw sample revealed scanty bacterial growth on the different media used on the first two days; however, there were observed increase in the microbial load from the third day through the seventh day. The highest number of microbial load 2.0 X 10^5 cfu/ml of colony was observed on the seventh day on nutrient agar (NA) medium while the lowest was 0.2 X 10^5cfu/ml on Eosin Methylene Blue Agar (EMB) respectively. No fungal growth was observed on Potato Dextrose Agar (PDA) medium as revealed in figure 1.

In the case of the cooked unwrapped walnuts, there was no bacterial growth on the different media for the first two days; however, there were scanty growth on the third day which increased with days till day seven. The highest number of bacterial load 1.9 X 10^5cfu/ml was observed on the seventh day on nutrient agar (NA) medium while the lowest was 0.4 X 10^4cfu/ml on day three on Mannitol Salt Agar. No fungal growth was observed on PDA medium as shown in figure 2.

Figure 3 showed the viable microbial load of the cooked wrapped walnut samples. There were no bacterial growth on the different media for the first two days, however, there were scanty and an increased bacterial load from day three through day seven. The highest bacterial load, 2.9 X 10^5cfu/ml was observed on the seventh day on nutrient agar (NA) media while the lowest was 1.0 X 10^4cfu/ml on day three and six on MSA media. However, no fungal growth was observed on PDA medium all through the seven days under investigation.

Biochemical identification of the isolated bacteria revealed six Gram negative organisms; *Pseudomonas spp, Pseudomonas aeruginosa, Salmonella spp, Citrobacter spp, Klebsiella spp,* and *Echerichia coli*; and four Gram positive bacteria; *Micrococcus spp, Staphylococcus spp, Bacillus spp,* and *Staphylococcus aureus* as shown in table 1.

Table 1: Biochemical Characteristics of the Isolated Bacteria

S/N	CODE	GR	L	GL	H2S	GAS	MOT	I	U	CIT	OX	CAT	COAG	MA	SF	SO
1	NA1	GNB	-	+	-	-	+	+	-	+	+	+	ND	ND	-	*Pseudomonas spp*
2	NA2	GPC	-	+	-	-	-	+	-	-	-	+	-	-	-	*Micrococcusspp*
3	NA3	GPC	-	+	-	-	-	ND	-	+	-	+	+	+	-	*Staphylococcus spp*
4	NA4	GPB	-	+	-	-	+	-	-	+	-	+	ND	-	+	*Bacillus spp*
5	NA5	GNB	-	+	-	-	+	-	-	+	+	+	ND	ND	-	*Pseudomonas aeruginosa*
6	MSA1	GPC	-	+	-	-	-	ND	-	+	-	+	+	+	-	*Staphylococcus aureus*
7	SSA1	GNB	-	+	+	-	+	-	-	+	-	+	ND	ND	-	*Salmonella spp*
8	EMB1	GNB	+	+	-	+	+	+	-	+	-	+	ND	ND	-	*Citrobacterspp*
9	EMB2	GNB	+	+	-	+	-	+	-	+	-	+	ND	ND	-	*Klebsiellaspp*
10	EMB3	GNB	+	+	-	+	+	+	-	-	-s	+	ND	ND	-	*Escherichia coli*

KEY:

NA = Nutrient Agar,
MSA = Mannitol Salt Agar,
SSA = Salmonella Shigella Agar,
EMB = Eosin Methylene Blue Agar,
GR = Gram Reaction,
GNB= Gram Negative *Bacilli*,
GPC= Gram Positive *Cocci*,
L = Lactose,
GL = Glucose,
H2S = Hydrogen Sulphide,
GAS = Gas Production,
MOT = Motility,
I = Indole,
U = Urease,
CIT= Citrate test,
OX = Oxidase,
CAT= Catalase,
COAG = Coagulase,
MA= Mannitol,
SF = Spore former,
SO = Suspected Organism.

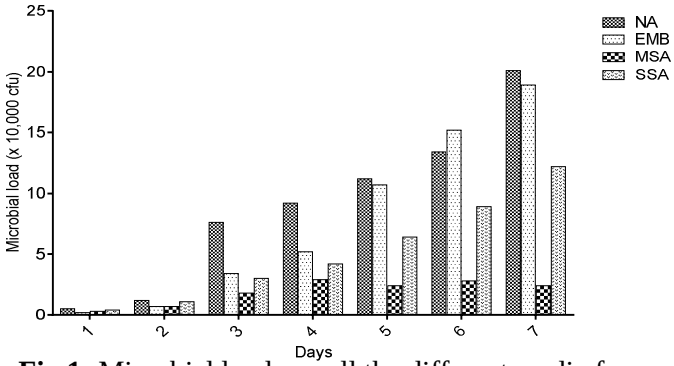

Fig.1: Microbial loads on all the different media for raw walnut.

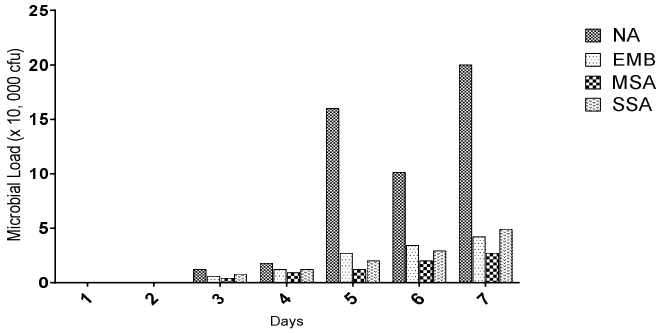

Fig. 2: Graph showing the microbial loads on different media for cooked unwrapped walnut**.**

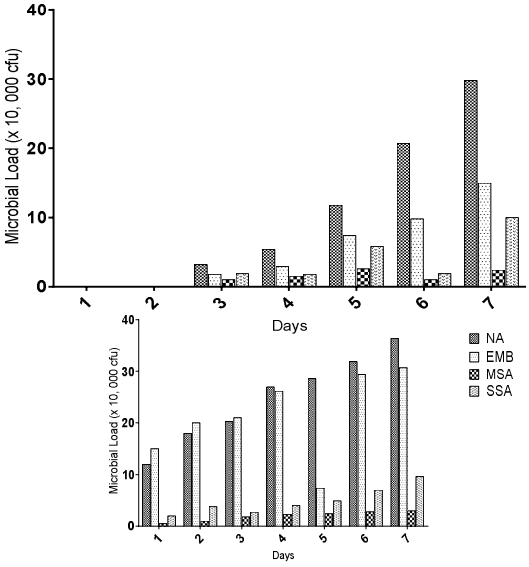

Fig. 3: Graph showing the microbial loads on different media for cooked wrapped walnut**.**

Fig. 4 Microbial loads on different media for hawker (1) walnut**.**

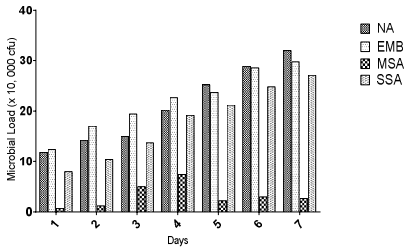

Fig. 5 Microbial loads on different media for hawker (2) walnut**.**

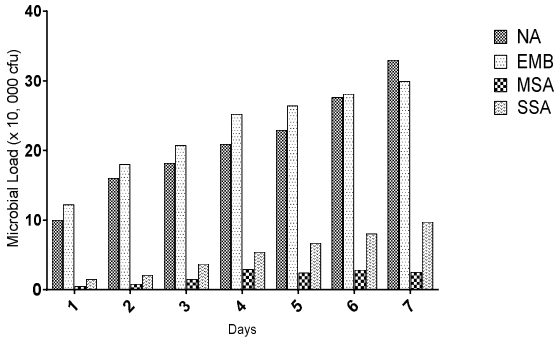

Fig. 6: Microbial loads on all the different media for hawker (3) walnut.

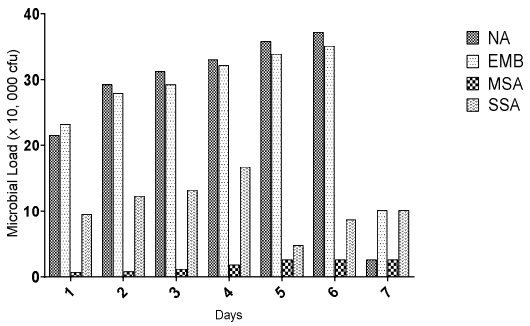

Fig. 7 Microbial loads on all the different media for hawker (4) walnut.

4.0 DISCUSSION

Fruits have the ability to be contaminated by microorganisms responsible for several human diseases when they are planted in field or during harvesting, transportation, processing, marketing and distribution or when stored in home (Issa-Zacharia *et al*., 2010). African Walnuts are generally known to have extremely high fat, protein and very low water content therefore they are susceptible to spoilage by bacteria (Ajewole *et al*., 2013; Arinola and Adeshina, 2014). Also, their storage can lead to the growth of mold under conditions that favors moisture. This study investigated the microorganisms responsible for potential spoilage of African walnut which were grouped into raw, cooked (both wrapped and unwrapped), and marketed (hawked).

In this study, eight different bacterial morphological characteristics (which include color, shape, edges, elevation, texture, surface appearance, transparency and size) were examined on five different growth media; Nutrient Agar (NA), Eosin Methylene Blue Agar (EMB), Salmonella Shigella Agar (SSA), and Mannitol Salt Agar (MSA). The Potato Dextrose Agar (PDA) had no fungal growth, hence there were no morphological characterization given in this work.

Biochemical identification of bacterial isolates suggested that enteric bacterial were the major microorganism found associated with the spoilt walnut and may be responsible for spoilage in African walnut. However, Ogwu *et al*., (2016) reported fungal growth for both fresh and cooked African walnut which may be due to longer duration of storage of the walnuts as the results obtained here, showed that within the period of the seven days observed, there were no fungal growth.

Some of the isolated bacteria in this study have been reported to be part of the natural flora of fruits or contaminants from the soil, washing or rinsing water, and from the environment during transportation or processing method (Ofor *et al*., 2009). For instance, *Pseudomonas spp* and *Bacillus spp* are known to be part of the natural flora of fruits responsible for spoilage (Issa-Zacharia *et al*., 2010). However, the identification of *Salmonella* spp, *Staphylococcus auerus* and *Klebsiella* indicates that there might be improper washing of the fruits leading to contamination of the fruits in the different groups been experimented.

The bacterial load in this study was reported using the NA because it showed the major bacterial count. The bacterial count was found to be very high in the hawked African walnut as shown in figures 4, 5 and 6 as compared to the raw and cooked samples shown in figures 1, 2 and 3. This may be due to storage condition or exposure to environmental factors such as high ambient temperature which might have favored bacterial proliferation.

These factors in addition to increased moisture content made possible by the nylon materials used for wrapping walnuts, and has provided a suitable condition for bacteria proliferation, might be responsible for the high bacterial load as reported for hawked samples, especially hawker-5, whose walnut had the highest bacterial load compare to other samples from the beginning as it was observed to be very wet throughout the experiment. Furthermore, it was discovered that the microbial load increased with time (days) which may be attributed to the low shelf life of the walnut in this study and was in line with the report of Ogwu *et al*., (2016).

5.0 CONCLUSION

Hawked African walnut is often highly contaminated and can readily be spoilt by bacteria as revealed by increased bacterial load in this research especially when hawked beyond two days.

There were presence of common bacterial causing human diseases such as *Pseudomonas spp, Staphylococcus spp, Staphylococcus aureus, Salmonella spp, Klebsiella spp*. *Bacillus spp* and *Escherichia coli* found in these nuts. Hence, proper measures should be taken in cleaning the African walnut prior to cooking, consumption and packaged for marketing.

RECOMMENDATION

Proper washing of African walnut with clean water after harvest before cooking be encouraged to remove all soil microorganisms from the shell of the nuts.

Hawking cooked walnuts beyond two days in nylon wraps should be discouraged in our

society by ensuring strict compliance to standards from regulatory bodies such as NAFDAC. Better storage method that will enhance longer walnut shelf life after cooking be put in place.

Despite the enormous health benefits of African walnuts, it remains a seasonal agricultural produce. Measures to ensure its all year round availability should be developed and encouraged.

CONFLICT OF INTEREST

The authors declared that there is no conflict of interest

ACKNOWLEDGEMENTS

The first author appreciates Mrs.Sobande, Agnes Olajumoke for being the inspiration behind this work. He thanks the Academic Staff Union of Nigerian Polytechnics (ASUP), Yaba College of Technology Chapter, for sponsoring the academic presentation of this work p. Also, my gratitude to all who were directly involved in the research team who made this work a success.

REFERENCES

Ajewole, K., Abibu, M.A. and Taleat, A.A. (2013). Proximate analysis of the edible part of the African walnut (*Juglans spiecie*). *Indian Journal of Natural products*. **9** (2): 51-54.

Akomolafe, S.F., Oboh, G., Akindahunnsi, A.A. and Afolayan, A.J. (2015a). Anti peroxidative activity of Tetracarpidium conophorum leaf extract in reproductive organs of male rats. *Evidence-Based Complementary and Alternative Medicine* 1–8.

Akomolafe, S.F., Oboh, G., Akindahunsi, A.A. and Afolayan, A.J. (2015b). Tetracarpidium conophorum ameliorates oxidative reproductive toxicity induced by ethanol in male rats. *Based Complementary and Alternative Medicine* **15**:439.

Akomolafe, S.F., Oboh, G., Akindahunnsi, A.A. and Afolayan, A.J. (2015c). *Tetracarpidium conophorum* (Mull. Arg) Hutch and Dalziel inhibit FeSO4 induced lipid per oxidation in rats genital. *Based Complementary and Alternative Medicine* **15**(57):1–11.

Akomolafe, S., Oboh, G., Olaseinde, T., Oyeleye, S. and Ogunsuyi, O. (2017a). Modulatory effects of aqueous extracts *Tetracarpidium conophorum* leaves on key enzymes linked to erectile dysfunction and oxidative stress induced penile lipid peroxidation in penile and testicular tissues. *Journal of Applied Pharmaceutical Sciences* **7**(1):51–56.

Arinola, S.O. and Adesina, K. (2014). Effect of thermal processing on the nutritional, antinutritional, and antioxidant properties of *Tetracarpidium conophorum* (African Walnut). *Journal of Food Processing*. 2014: 1-4.

Ayoola, P. B., Adeyeye, A., Onawumi, O. O. and Faboya, O. O. P. (2011) . Phytochemical and nutrient evaluation of *Tetracarpidium conophorum* Root. *International Journal of Research and Reviews in Applied Sciences*. **7**(2): 197 – 202.

Dada, A. and Aguda, O. (2015). Dietary effects of African walnut (*Tetracarpidium conophorum*) on the reproductive indices in male African catfish (*Clarias gariepinus*) broodstock. *Journal of Coastal Life Medicine* 3(6):471–475.

Dauda, A. O., Abiodun, O. A., Akintayo. O. A., Babayeju, A. A., Salami, K. O. and Oyekanmi, I. A. (2020). Influence of walnut on the nutritional and physicochemical properties of biscuits made from whole wheat *Agrosearcch*, 20(1): 45-58.

Ikpeme, E.V., Ekaluo, U.B., Udensi, O., Ekerette, E.E., Ekpo, P.B. and Asuquo, B.O.(2014). Sperm quality and hormone profile of male albino rats fed with seeds of African walnut (*Tetracarpidium conophorum*, Mull), *Annual Research & Review in Biology* **4**(9):1379–1386.

Issa-Zacharia, A., Kamitani, Y., Muhimbula, H.S. and Ndabikunze, B.K. (2010). A review of microbiological safety of fruits and vegetables and the introduction of electrolyzed water as an alternative to sodium hypochlorite solution. *African Journal of Food Science* 4(13): 778 - 789.

Kanu, A.M., Kalu, J.E., Okorie, A.C., Olabinri, B.M., Eniyansoro, O.O. and Okoronkwo, C.O. (2015). 'Evaluation of chelating ability of aqueous extract of *Tetracarpidium conophorum* (African walnut) in vitro. *International Journal Applied Research in Natural Products* **3**(3):1–13.

Nwachoko, N. and Jack, I.R. (2015). Phytochemical screening and anti-diarrhea activities of *Tetracarpidium conophorum* induced in albino rats. *Journal of Biochemistry Research* 4(4):21–24.

Ofor, M.O., Okorie, V.C., Ibeawuchi, I.I., Ihejirika, G.O., Obilo, O.P., Dialoke, S.A.(2009). microbial contaminants in fresh tomato wash water and food safety considerations in South-Eastern Nigeria. *Life Sci. Journal*, 1:80-82.

Ogbonna, O.J., Udia, P.M., Takem, L.P., Ogbeihe, G.O. and Onyekpe, P.I. (2013) . Comparative antidiabetic effects of leaf and root extracts of *Tetracarpidium conophorum* and oral hypoglycemic agents on alloxan-induced diabetic rats. *International Journal of Pure and Applied Sciences and Technology* **19**(1): 82–87.

Ogbonna, O.J., Udia, P.M., Ikechi, W.N., Ogbeihe, G.O., Omoregha, C.U. and Nnaemeka, L.B.(2015). Effect of root and leaf extracts of *Tetracarpidium conophorum* on liver enzyme levels in alloxan-induced diabetic rats. *British Journal of Pharmaceutical Research* **5**(4): 241–248.

Ogunyinka, B.I., Oyinloye, B.E., Adenowo, A.F. and Kappo, A.P. (2015). Potentials of some plant-derived foods in the management of diabetes and associated complications. *African Journal of Traditional Complementary and Alternative Medicines* 12(6):12–20.

Ogwu, M. C., Osawaru, M. E. and Atsenokhai, E. I. 2016. Chemical and microbial evaluation of some uncommon indigenous fruits and nuts. Borneo Science 37 (1): 54-71.

Olaniyi, F.E., Bamidele, I.O., Omokehinde, A.O. and Ayodeji, A.A. (2016). Anti-inflammatory activities of the chloroform extract of the fruit of *Tetracarpidium conophorum* (Mull. Arg.) (Nigeria Walnuts). *Journal of Advance in Medical and Pharmaceutical Sciences* 6(1): 1–7.

Onwuli, D.O., Bown, H. and Ozoani, H.A. (2014). Anti-hyperglycemic effect of *Tetracarpidium conophrum* in alloxan induced diabetic female albino rats. Endocrinology 1:4-7

Pan, A.N., Sun, Q.I., Manson, J.E., Willett, W.C. and Hu, F.B. (2013). Walnut consumption is associated with lower risk of type 2 diabetes in Women. *Journal of Nutrition* 1**43**(4):512–518.

MHD FLOW OF DOUBLE-DIFFUSIVE CONVECTION WITH CONVECTIVE BOUNDARY CONDITIONS IN THE PRESENCE OF CHEMICAL REACTION AND THERMAL RADIATION

Esan O. A, **Baiyeri** J.F, **Ogunbayo** T.O, and **Mohammed** M.A

Department of mathematics, Yaba College of Technology Yaba, Nigeria.
Corresponding author's Email: *baiyeri.funsho@gmail.com*

ABSTRACT

The study analyzed magnetohydromagnetic (MHD) boundary layer flow of convective double diffusion over a flat sheet in the existence of radiation, chemical reaction and heat source. Applying similarity variables, the main modelled equations governing the flow are reduced to couple derivative of nonlinear order. The obtained system of equations is computationally solved by fourth-other Runge-Kutta techniques alongside with shooting Nachtsheim-Swigert schemes. The effect of some embedded physical terms on the heat and flow momentum is examined and discussed. The numerical results for heat and species gradients, and skin friction are also gotten. The embedded fluid flow parameters have a significant impact on the wall surface. Interestingly, the combined effects of the embedded fluid flow parameters could be used in designing our physical complex flow systems.

KEYWORDS:

Chemical reaction; MHD flow; Double-diffusive convection; Thermal radiation; Heat generation

1.0 INTRODUCTION

In several natural phenomena, heat and species diffusion occur simultaneously to generate a buoyancy force that propels liquid flow which is described as double diffusive. This also defines the flows driven by diverse density gradients with different diffusion rate as reported by Akbar et al. (2016). In oceanography, processes involving convection of salinity and temperature gradients are called thermohaline convection, meanwhile, the temperature surface gradients and the species molecular diffusion are called Marangoni convection. The processes that embroils the combined species mass and thermal gradients utilized double-convective diffusion which is widely used to examine several natural phenomena. Due to the relationship between the fluid diffusion and the velocity fields, convective double-diffusion is highly intricate than the single-diffusive convection, Kareem and Salawu (2017). As such, double-diffusion process take place in different fields which includes chemical engineering (evaporation, gas liquefaction, thin films deposition, sublimation, drying, cleaning operations, salt caverns solution mining and more), condensed physics (crystal growth, alloy binary solidification), oceanography (earth crust crystallization igneous, ice surface cooling and melting, intrusion of sea-lake water), geophysics (flow matter particulate or materials dissolvent dispersion), etc.

An insight to the interaction nature between concentration and energy buoyancy forces are essential in order to understand and manage its effect, Olanrewaju et al. (2013). Heat convective transport in permeable media is of great interest to the scientist and researchers some decades due to their importance in ground hydrology, mining, aquifers pollutant dispersion, geophysical, electronic systems cooling, room ventilation, reactors chemical catalysis, crystal liquid growth, petroleum reservoirs and others, Bejan et al. (2004) and Dada and Salawu (2017). The heat-transfer analysis of boundary-layer flows with radiation is also important in electrical power generation, astrophysical flows, solar power technology, space vehicle re-entry and other industrial areas, Baiyeri et al. (2017). Extensive literature that deals with flows in the presence of radiation effects is now available,

Olanrewaju et al. (2011); Salawu and Amoo (2016). Ishak (2010) stated that heat convective transport analysis is imperative to the high temperature processes, such as energy thermal storage, nuclear plants and gas turbines. Fluids binary mixture of boundary layer flow are of great usefulness to the pharmacy and chemical engineering. As such, Okedoye and Salawu (2019) examined MHD binary chemical reaction in an oscillatory moving boundary layer surface with heat and mass reaction. The significant of binary species reaction was reported in the study. Moreover, many chemical processing industries are considered to transmute raw materials to valuable produces by the chemical reaction process. A device where chemical mixture takes place creates contact relation by providing suitable species concentration and heat fields throughout the process Salawu and Amoo (2016).

Fluid dynamics demonstrates an essential role in the flow of radiative chemical reaction diffusion with energy transfer, which established the correlation between the reactor performance and hardware. Subhashini et al. (2011) examined convective double-diffusive of chemical species flow over a porous vertical plate with convective border conditions. Mohamed (2009) considered unsteady convective MHD reaction double-diffusive of flowing fluid past a moving vertical permeable sheet with radiation, soret effects and heat generation. Coupled thermal and momentum boundary layer flow of similarity solutions with heat transfer and convection was examined by Incropera et al. (2007); Yadav and Agrawal (2013). Cheg (2009) studied in a porous vertical truncated device, the analysis variable viscosity of boundary layer flow of convective double-diffusion using similarity transformation. Most recently, Abdelraheem et al. (2018) discussed the natural convection of double-diffusive nanofluid flow in a square cavity permeable plate with sinusoidal distributions. More also, Mohamad (2004); Yang et al. (2013) analyzed the natural convective flow of reactive double-diffusion in a filled enclosed porous rectangular device with saturated binary fluid. The problem was numerically solved and parametric sensitivity analysis was reported. Recently, Gaikwad, SN & Kamble, SS. (2016) discussed the effects of the cross diffusion of a couple stress liquid on a convective double-diffusive reaction with anisotropic rotating saturated permeable layer.

The major aim of the current study is to examine the flow pattern, energy and species concentration transfer of convective double-diffusive fluid flow past a flat plate surface with surface convective boundary conditions. The reaction process occurs in the presence of thermal radiation, chemical reaction and heat generation. The study is motivated by the significant results obtained by previous analysis carried out and the importance of the double-diffusion to the industry and technological advancement. To the best of the author's knowledge, the combined influences of species reaction, heat generation and radiation with other embed flow parameters have not been investigated with surface convective boundary condition.

2.0 MATHEMATICAL FORMULATION

Consider a steady non-single dimensional flow of laminar, conductive, incompressible mass concentration reaction liquid stimulated by convective buoyancy forces. The flowing fluid in a vertical porous device is exposed to convective boundary cooling to prevent the fluid molecular deformation as a result of reaction diffusion. The fluid far stream temperature T_∞ is stirring past the plate right surface with unvarying flow rate U_∞ while the plate left surface is wide-open to convective heating by the heated liquid temperature T_f that provide a coefficient heat transfer. The buoyancy force arises due to the variation in the temperature and mass species of the liquid. The induced electromagnetic field is neglected due to the absence of magnetic field and the Reynolds number is ignored. As such, the fluid flow is not electrically conducting as demonstrated in Figure 1.

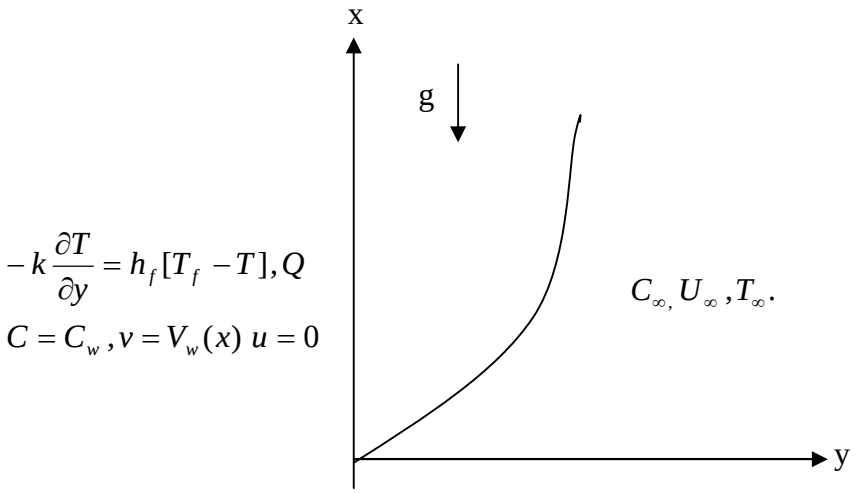

Figure 1: Geometry of the flow model

The mass conservation, velocity component, energy and mass equations defining the flowing fluid is written as, Olanrewaju, et al [2];

$$\frac{\partial u}{\partial x}+\frac{\partial v}{\partial y}=0 \tag{1}$$

$$u\frac{\partial u}{\partial x}+v\frac{\partial u}{\partial y}=\upsilon\frac{\partial^2 u}{\partial y^2}+g\beta\left(T-T_\infty\right)+g\beta^*\left(C-C_\infty\right) \tag{2}$$

$$u\frac{\partial T}{\partial x}+v\frac{\partial T}{\partial y}=\alpha\frac{\partial^2 T}{\partial y^2}+\alpha\left(\frac{\partial u}{\partial y}\right)^2+\frac{Q}{\rho c_p}\left(T-T_\infty\right)-\frac{\alpha}{k}\frac{\partial q_r}{\partial y} \tag{3}$$

$$u\frac{\partial C}{\partial x}+v\frac{\partial C}{\partial y}=D\frac{\partial^2 u}{\partial y^2}-R\left(C-C_\infty\right)^n \tag{4}$$

Alongside with boundary conditions

$$u(x,0)=0,\ v(x,0)=V_w(x),\ \ -k\frac{\partial T}{\partial y}(x,0)=h_f[T_f-T(x,0)],\ \ C=C_f \tag{5}$$

$$u(x,\infty)\to U_\infty,\ C(x,\infty)\to C_\infty,\ T(x,\infty)\to T_\infty \tag{6}$$

where u and v are respectively the flow rate components, T is the temperature, g is the gravitational, β^* is the coefficient of solutant expansion, α is the heat diffusivity, υ is the kinematic viscosity of the fluid, β is the coefficients of heat expansion, k is the heat conductivity, Q is the heat release, q_r is the radiative heat flux, D is coefficient of species diffusivity and R is the chemical reaction.

The radiative thermal flux q_r through Rosseland approximations is given by [9]

$$q_r = -\frac{4\sigma_r}{3k_e}\frac{\partial T^4}{\partial y}, \tag{7}$$

where σ_r is the Stefan-Boltzman constant with k_e be the mean absorption. With small temperature differences, equation (7) is linearized by expanding T^4 using Taylor series in T_∞. On ignoring higher order terms, the expansion gives

$$T^4 = 4T_\infty^3 T - 3T_\infty^4 \tag{8}$$

Using equations (7) and (8), equation (3) becomes

$$u\frac{\partial T}{\partial x} + v\frac{\partial T}{\partial y} = \alpha\frac{\partial^2 T}{\partial y^2} - \frac{16\sigma_s T_\infty^3}{3k_e\rho c_p}\frac{\partial^2 T}{\partial y^2} + \frac{Q}{\rho c_p}(T - T_\infty) + \alpha\left(\frac{\partial u}{\partial y}\right)^2 \tag{9}$$

Here we introduce the a transformation variable η and a non-dimensional stream function f(η), θ(η) and φ(η) as

$$\eta = y\sqrt{\frac{U_\infty}{\upsilon x}},\ \psi = \sqrt{\upsilon v U_\infty}\, f(\eta),\ \theta(\eta) = \frac{T - T_\infty}{T_w - T_\infty},$$

$$\phi(\eta) = \frac{C - C_\infty}{C_w - C_w}, u = U_\infty f'(\eta),\ v = \frac{1}{2}\sqrt{\frac{\upsilon U_\infty}{x}}(\eta f' - f). \tag{10}$$

Equation (1) is automatically fulfilled and equations (2)-(9) can be transformed to the subsequence dimensionless forms after some manipulations to give the following equations

$$f''' + \frac{1}{2}ff'' + Gr\,\theta + Gr_C\phi = 0 \tag{11}$$

$$\left(1 + \frac{4}{3}Ra\right)\theta'' + \frac{1}{2}\Pr\, f\theta' + \Pr\,\beta\theta + \Pr\, Ec(f''^2) = 0 \tag{12}$$

$$\phi'' + \frac{1}{2}Scf\phi' - Sc\lambda\phi = 0 \tag{13}$$

Satisfying the boundary conditions

$$f(0) = f_w, \quad f'(0) = 0, \quad \theta'(0) = -Bi[1 - \theta(0)] \quad \phi(0) = 1$$
$$f'(\infty) = 1 \quad \theta(\infty) = 0 \quad \theta \to 0 \quad \phi(\infty) = 0 \tag{14}$$

where primes depict derivative with respect to η and the terms seeming in equations (11-14) are the embedded fluid flow parameters. Gr, Grc, Ra, Pr, β, Ec, Sc, λ, f_w, and B_i represents the local heat Grashof number, local solutal Grashof number, radiation term, Prandtl number, internal heat generation, Eckert number, Schemitl number, species reaction term, suction term and convective Biot number. It is evident that the computed solutions is binding in as much its denote local similarity solutions since the terms depends on the independent variable x.

2.1 NUMERICAL PROCEDURE

In the current analysis, the set of equations (11), (12) and (13) with the boundary conditions of equation (14) are solved computationally by using shooting Nachtsheim-Swigert scheme coupled with integrating fourth-order Runge-Kutta technique. Taking from the computation

process, the coefficient skin-friction, heat gradient number and local mass gradient number, are presented as $f''(0), -\theta'(0)$ *and* $-\phi'(0)$. The computed numerical results are offered in table. The numerical solutions is carried out via a computer symbolic language MAPLE (Olanrewaju, et al. [4]).

A step size of $\Delta\eta = 0.001$ is chosen for a suitable convergence measure of 10^{-10} for almost all cases. The value of y_∞ is obtained for each loop of iteration by taken $\eta_\infty = \Delta\eta + \eta_\infty$. The highest value of η_∞, for each term, Pr, Gr, Grc, Ra, Ec, Sc, Bi, λ, β, and f_w are evaluated for the unknown boundary conditions at $\eta = 0$ for error loop 10^{-10}.

3.0 ANALYSIS OF THE RESULTS

In order to get a clear insight of the physical problem, the velocity, temperature and concentration have been discussed by assigning numerical values to the parameters encountered in the problem. To be realistic, the values of Schmidt number (Sc) are chosen for hydrogen (Sc = 0.22), water vapour (Sc = 0.62), and Propyl Benzene (Sc = 2.62) at temperature 25^{o}C and one atmospheric pressure. The values of Prandtl number is chosen to be Pr = 0.72 which represents air at temperature 25^{o}C and one atmospheric pressure. Attention is focused on positive values of the buoyancy parameters i.e. Grashof number $G_r > 0$ (which corresponds to the cooling problem) and solutal Grashof number

$G_m > 0$ (which indicates that the chemical species concentration in the free stream region is less than the concentration at the boundary surface). In table 1, we generate the skin friction coefficient, Nusselt number and the Sherwood number for some embedded flow parameters value in the flow model. Here, when the Prandtl number Pr increases, the Skin-Friction coefficient increase with the heat transfer at the wall surface (local Nusselt number) while the mass transfer rate at the wall surface decreases across the channel. Similarly, when the thermal Grashof number Gr increases, the Skin-Friction coefficient and the local Nusselt number increases while the local Sherwood number decreases. It was observed that when the Solutal Grashof number Gc, thermal radiation parameter Ra and the internal heat generation parameter β increases, the Skin-friction coefficient and heat transfer rate increases while the mass transfer rate increases. It was also noticed that when the Schmitt number Sc and the chemical reaction parameter λ increases, the Skin-friction coefficient, heat transfer rate and the mass transfer rate at the wall increases. It implies that the Schmitz number and the chemical reaction parameters enhance the skin-friction coefficient, mass transfer rate and the heat transfer rate at the wall surface. We also observed that as the suction parameter fw, Eckert number Ec and the Biot number Bi increases, the skin-friction coefficient decreases while the heat and mass transfer rate at the wall decreases. Finally, the injection parameter fw <0 increases, the skin-friction coefficient increases while the heat and mass transfer rate at the wall surface decreases. It is also observed that injection increases the fluid flow while suction reduces the fluid flow velocity.

Figure 2 depicts the solution of temperature against η for various values of Prandtl numbers Pr and it is observed that increasing Pr decreases the thermal boundary layer thickness across the flow channel. Figure 3 depicts the plot of concentration against η for various values of the thermal Grashof number. It is clearly seen from the figure that increases in the thermal Grashof number increases the velocity boundary layer thickness. In figure 4, it can be seen that the same effect occurs as in figure 2. Increasing the solutal Grashof number increases the velocity boundary layer thickness as exthickness. Increasing the radiation parameter Ra thickens the thermal boundary layer thickness apected. Figure 5 shows the influence of radiation parameter Ra on the thermal boundary layer cross the flow channel. In figure 6, we represent the graph of the velocity against η for various values of Eckert number Ec. It was observed that an increase in the Eckert number bought a slight increase in the velocity profile close to the wall surface. Figure 7 represents the temperature distribution against η for various values of the Eckert number. We established that increase in the Eckert number thickens

the thermal boundary layer across the flow channel. Similarly, it was discovered that Eckert number enhances the thermal boundary layer thickness. The effect of Schmidt number Sc on the concentration profile is presented in figure 8. Increasing Sc is to decrease the concentration boundary layer thickness. In figure 9, we discovered that as the Biot number Bi increases, the temperature boundary layer thickness thickens and therefore the thermal boundary layer thickness increases. Figures 10 – 12 represents the graph of concentration distribution against η for various values of chemical reaction parameters. For a destructive chemical reaction parameter, the concentration boundary layer thickness thins across the flow channel while for the additive reaction parameters; the concentration boundary layer thickness thickens. In figure 13, we plot the graph of temperature against η for various values of internal heat generation parameter β. It was observed that as we this parameter increases, the thermal boundary layer thickness thickens across the flow channel. Figure 14 represents the solution of velocity against η for various values of the injection parameter fw >0. It was discovered that as injection parameter increases, the flow rate also increases which resulted in the thickening of the velocity boundary layer thickness. In figure 15, we noticed that when we increase the suction parameter fw <0, the concentration boundary layer thickness decreases which alternatively step down the rate of flow. In figures 15 and 17, the effect of wall porosity term fw on the flow velocity, concentration and temperature are presented. The momentum, mass and thermal boundary layer thickness decreases and increases with the rising parameter values. Finally, in parameter analysis, the choice of parameters is of high value in order to get the expected results or valuable results in mathematical modeling (see Ingham and Pop [16]).

Table 1: Computation showing $F''(0)$, $\theta'(0)$ and $\phi'(0)$ for various values of embedded fluid flow parameters

Gr	**Gc**	**Ra**	**Ec**	**Sc**	**Bi**	λ	β	$-F''(0)$	$-\theta'(0)$	$-\phi'(0)$
0.5	0.5	0.1	0.1	0.62	0.1	0.1	0.1	-1.22712658	0.0709929717	0.5220851259
0.5	0.5	0.1	0.1	0.62	0.1	0.1	0.1	-1.20722422	0.0722601926	0.5202229040
0.5	0.5	0.1	0.1	0.62	0.1	0.1	0.1	0.25985882	0.2105628793	0.3350501163
0.6	0.5	0.1	0.1	0.62	0.1	0.1	0.1	-1.2592271	0.0708278466	0.5241385115
0.7	0.5	0.1	0.1	0.62	0.1	0.1	0.1	-0.4118728	0.0998754124	0.3434014214
0.5	0.6	0.1	0.1	0.62	0.1	0.1	0.1	-1.32183366	0.0705084379	0.5277687974
0.5	0.61	0.1	0.1	0.62	0.1	0.1	0.1	-1.33118948	0.0704576559	0.5283204405
0.5	0.5	0.3	0.1	0.62	0.1	0.1	0.1	-1.24204196	0.0700047367	0.5234954846
0.5	0.5	0.5	0.1	0.62	0.1	0.1	0.1	-1.25571233	0.0690879353	0.5247971033
0.5	0.5	1.0	0.1	0.62	0.1	0.1	0.1	-1.28580376	0.0670692103	0.5276853936
0.5	0.5	0.1	0.5	0.62	0.1	0.1	0.1	-1.49591186	0.0236523233	0.5388820477
0.5	0.5	0.1	1.0	0.62	0.1	0.1	0.1	-2.09533148	-0.095640680	0.5714089683
0.5	0.5	0.1	0.1	1.0	0.1	0.1	0.1	-1.14998469	0.0714760822	0.6699445045
0.5	0.5	0.1	0.1	2.62	0.1	0.1	0.1	-1.00886268	0.0720994833	1.1715903070
0.5	0.5	0.1	0.1	0.62	0.1	0.5	0.1	-1.16020160	0.0714035408	0.7198636838
0.5	0.5	0.1	0.1	0.62	0.1	0.1	0.5	-1.66617087	0.0055483427	0.5514562371

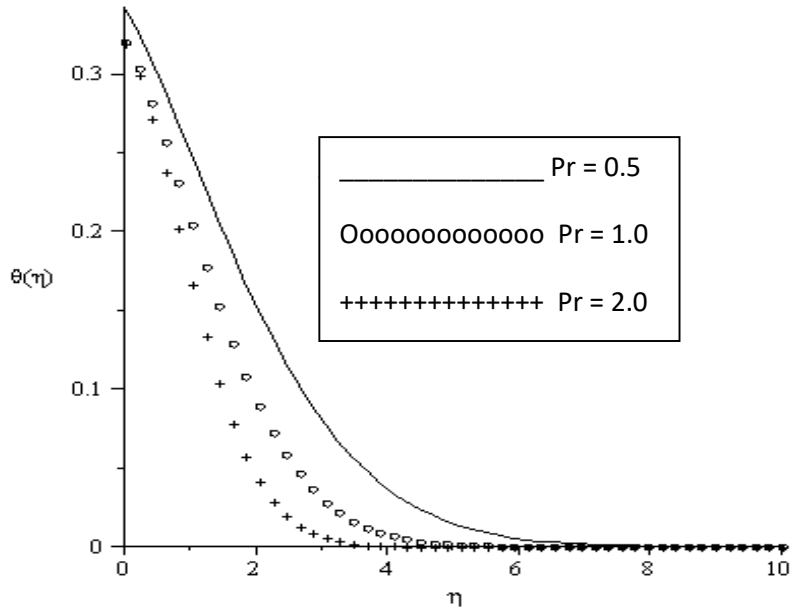

Figure 2: Temperature distribution of various values of Prandtl number Pr with fixed values of **Gr = Gc = Ra = fw = 0.5, Ec = Sc = Bi =** $\lambda = \beta$ **= 0.1**

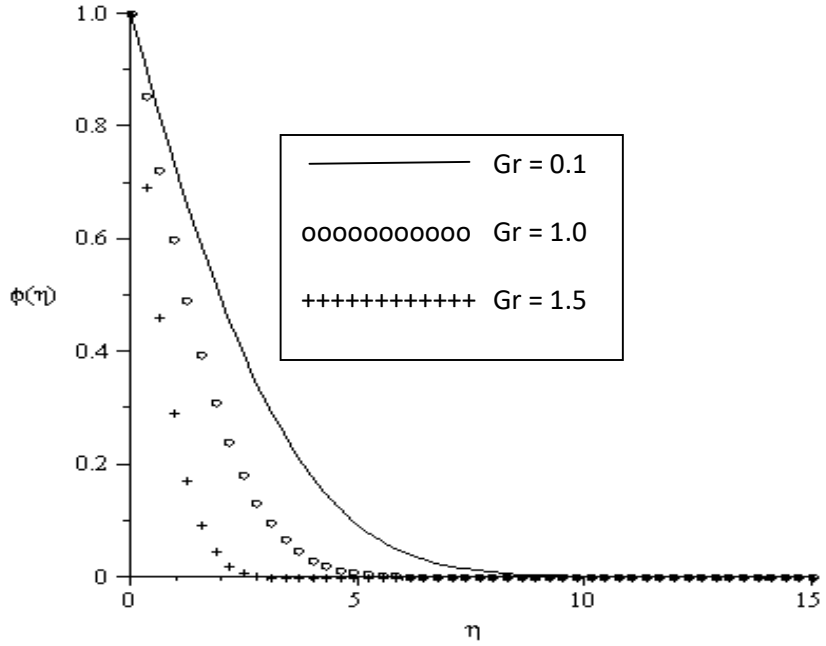

Figure 3: Concentration distribution for various values of thermal Grash of number Gr with fixed values of **Gc = Ra = Ec = Sc = Bi =** $\lambda = \beta$ **= Pr = 0.1. fw = 0.5**

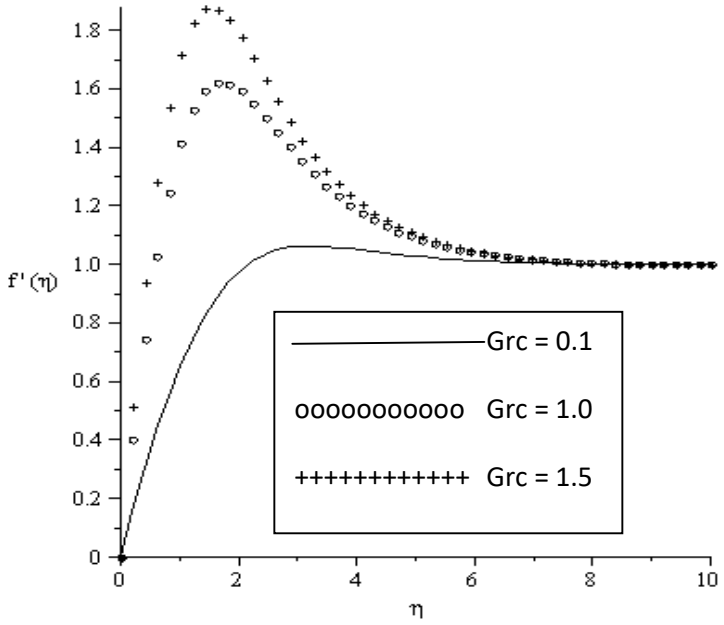

Figure 4: Velocity distribution for various values of solutal Grash of number Gc with fixed values of **Gr = Ra = Ec = Sc = Bi =** $\lambda = \beta$ **= Pr = 0.1. fw = 0.5**

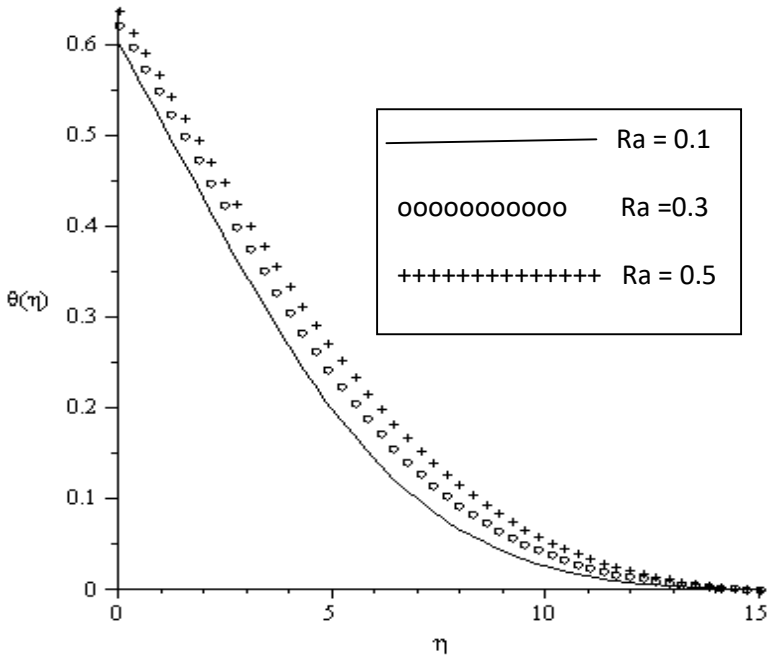

Figure 5: Temperature distribution for various values of radiation parameter Ra for fixed values of **Gr= Ec = Sc = Gc =** $\lambda = \beta$ **= Pr = 0.1. Bi = 0.2, fw = 0.5**

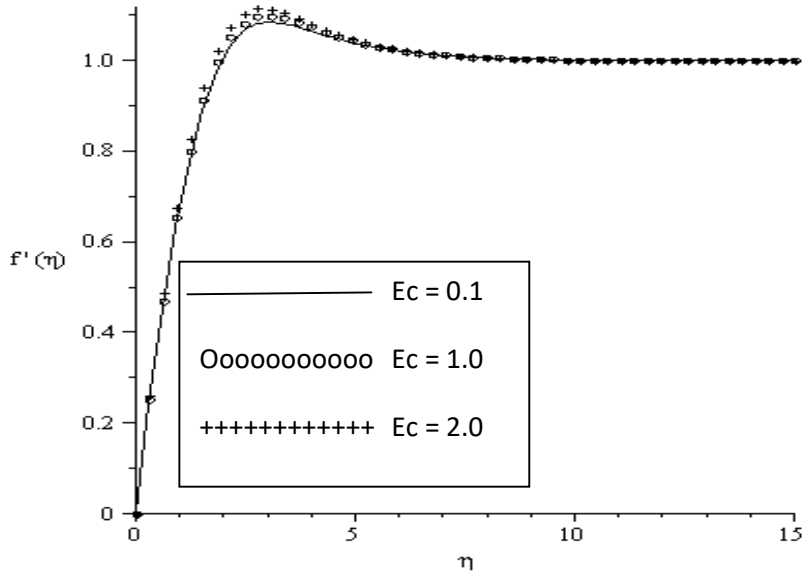

Figure 6: Velocity distribution for various values of Eckert number Ec for fixed values of **Gr= Ra = Sc = Gc =** λ = β = **Pr = 0.1. Bi = 0.2, fw = 0.5**

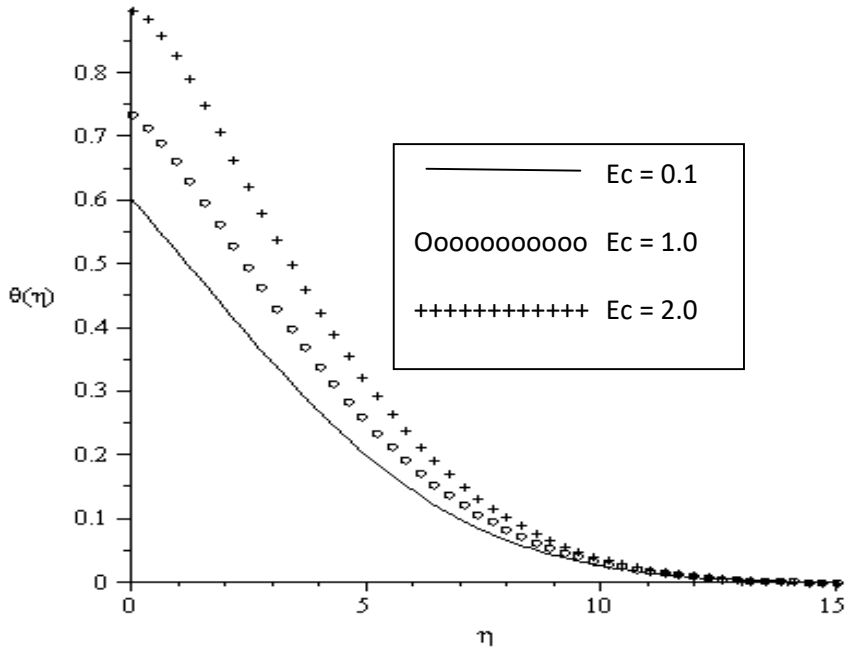

Figure 7: Temperature distribution for various values of Eckert number Ec for fixed values of **Gr= Ra = Sc = Gc =** λ = β = **Pr = 0.1. Bi = 0.2, fw = 0.5**

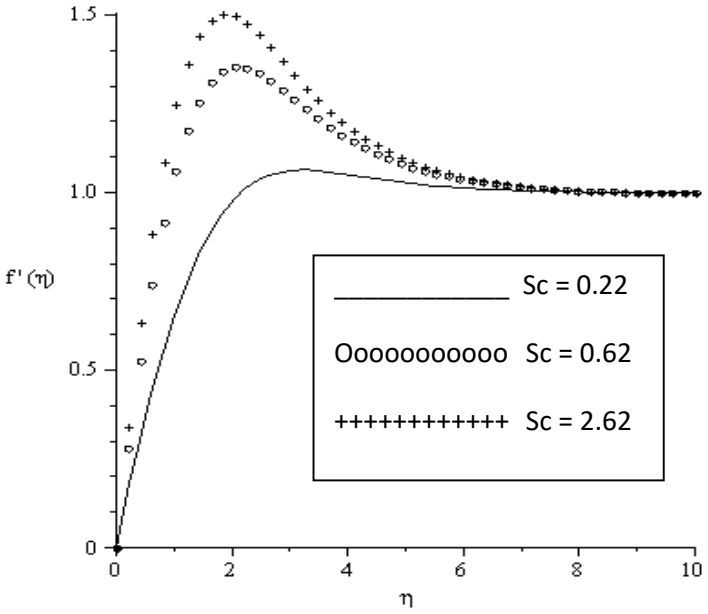

Figure 8: Concentration distribution for various Schmitz number Sc for fixed value of **Gr= Ra = Ec= Gc =** λ = β = **Pr = 0.1. Bi = 0.2, fw = 0.5**

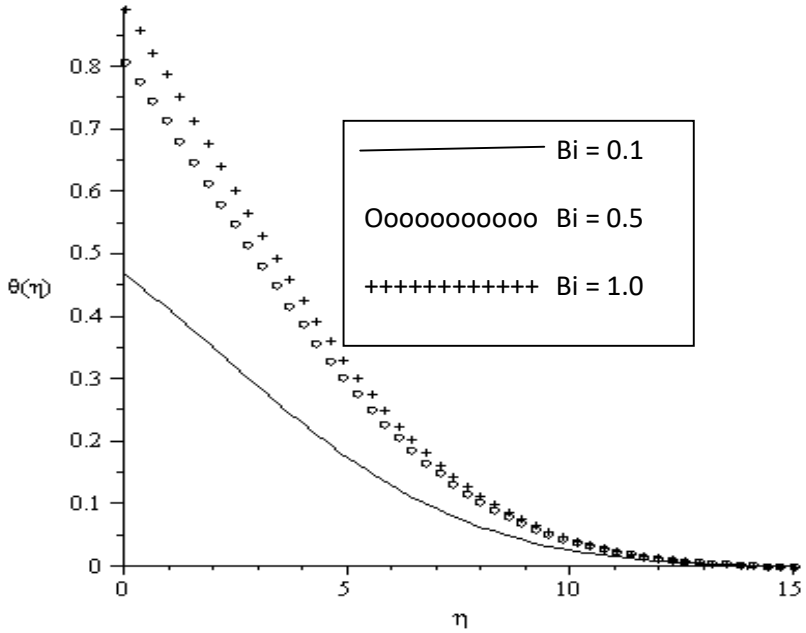

Figure 9: Temperature distribution for various values of Biot number Bi for fixed values of **Gr= Ra = Ec= Gc =** λ = β = **Sc = 0.1. Pr = 0.1, fw = 0.5**

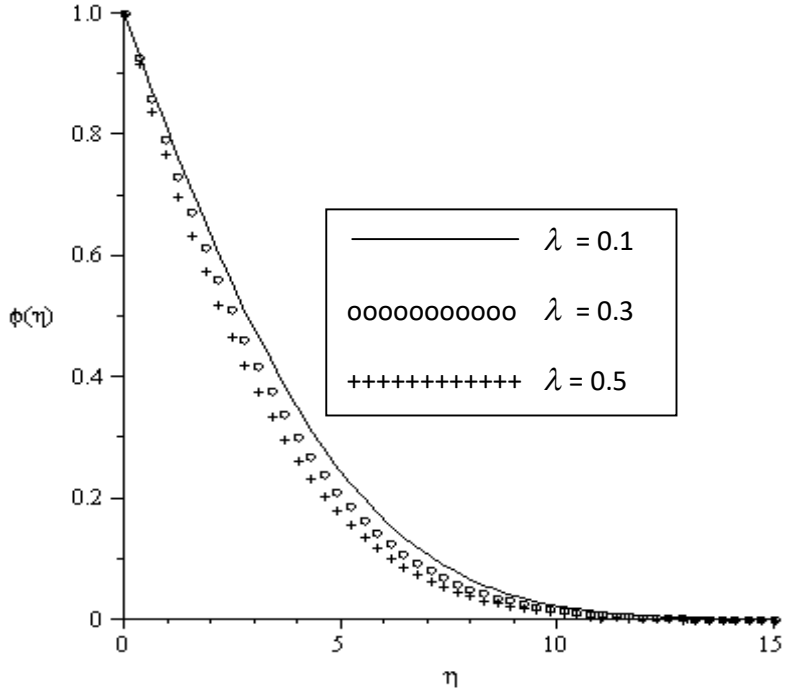

Figure 10: Concentration distribution for various values of chemical reaction parameter λ for fixed values of **Gr= Ra = Ec= Gc = Bi =** β **= 0.1. Pr = 0.1, fw = 0.5**

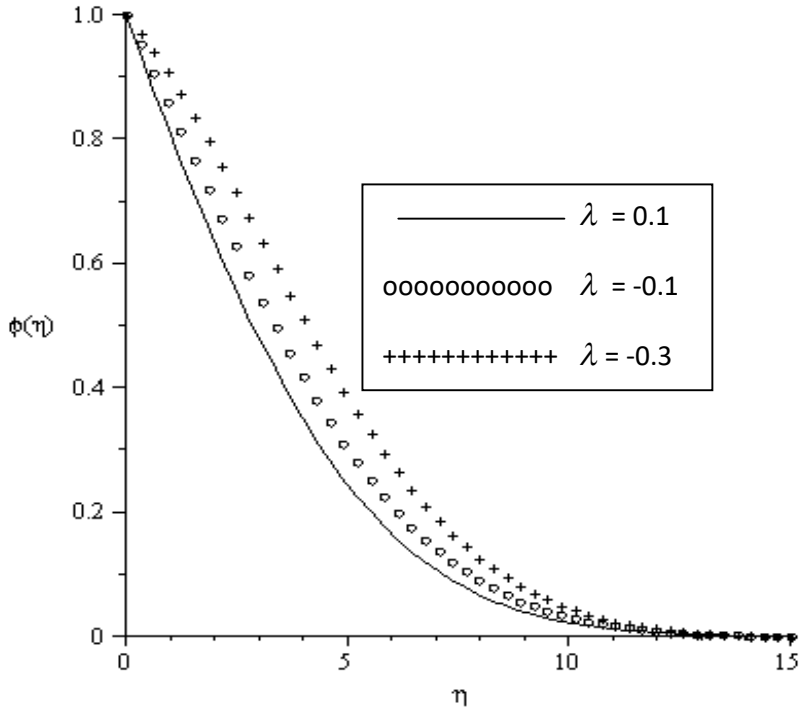

Figure 11: Concentration distribution for various values of chemical reaction parameter λ for fixed values of **Gr= Ra = Ec= Gc = Bi =** β **= 0.1. Pr = 0.1, fw = 0.5**

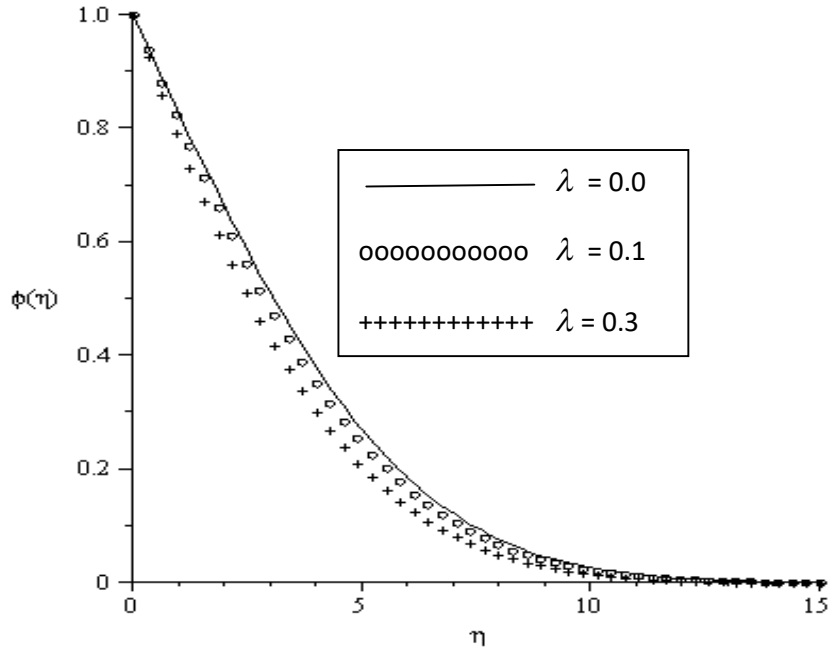

Figure 12: Concentration distribution for various values of chemical reaction parameter λ for fixed values of **Gr= Ra = Ec= Gc = Bi =** β **= 0.1. Pr = 0.1, fw = 0.5**

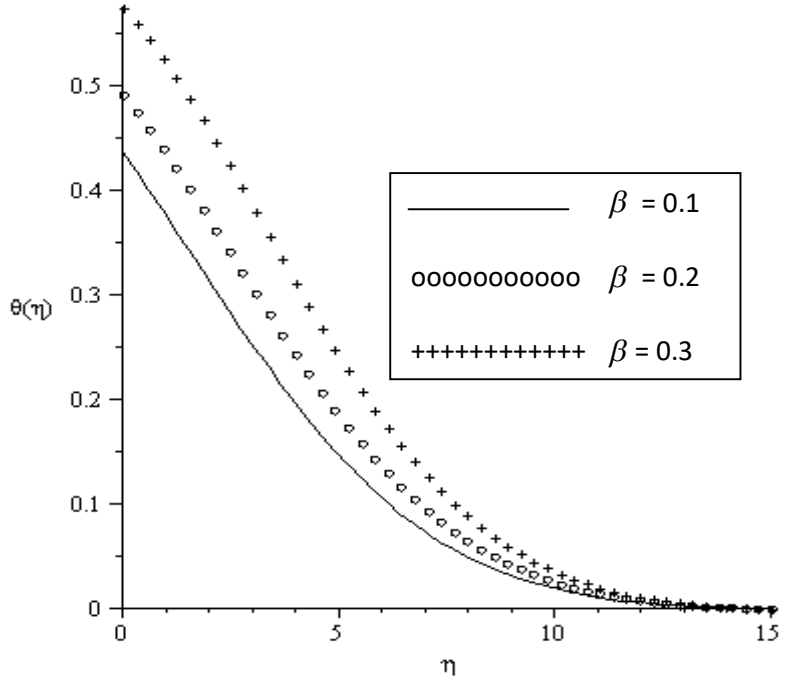

Figure 13: Temperature distribution for various values of internal heat generation parameter β for fixed values of **Gr= Ra = Ec= Gc = Bi = Sc = 0.1. Pr = 0.1, fw = 0.5,** λ **= 0.1**

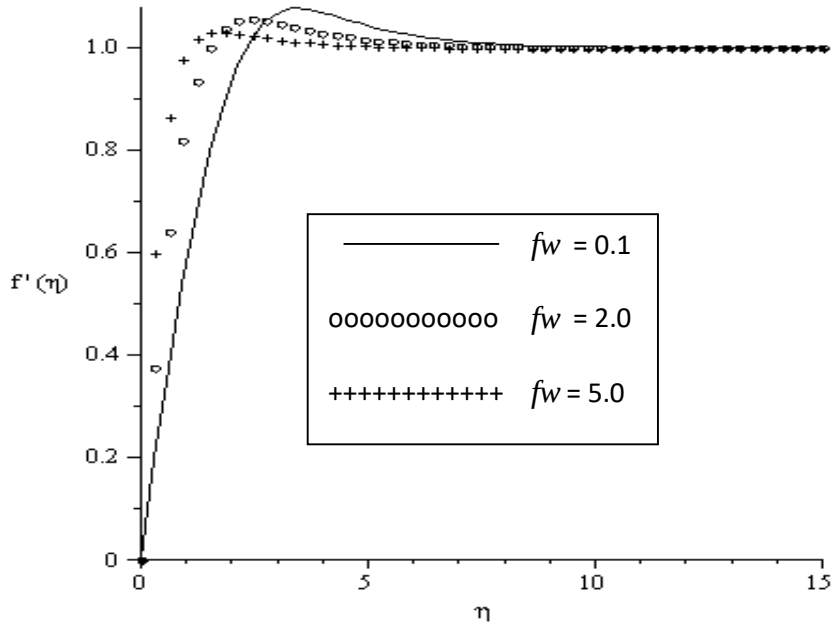

Figure 14: Velocity distribution for various values of suction parameter fw for various values of **Gr= Ra = Ec= Gc = Bi = Sc = 0.1. Pr = 0.1,** β **= 0.1,** λ **= 0.1**

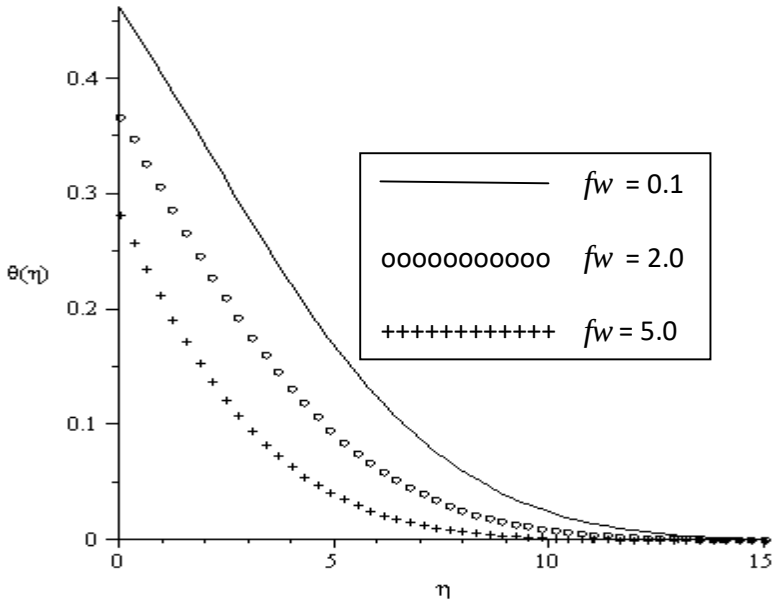

Figure 15: Temperature distribution for various values of suction parameter fw for various values of **Gr= Ra = Ec= Gc = Bi = Sc = 0.1. Pr = 0.1,** β **= 0.1,** λ **= 0.1**

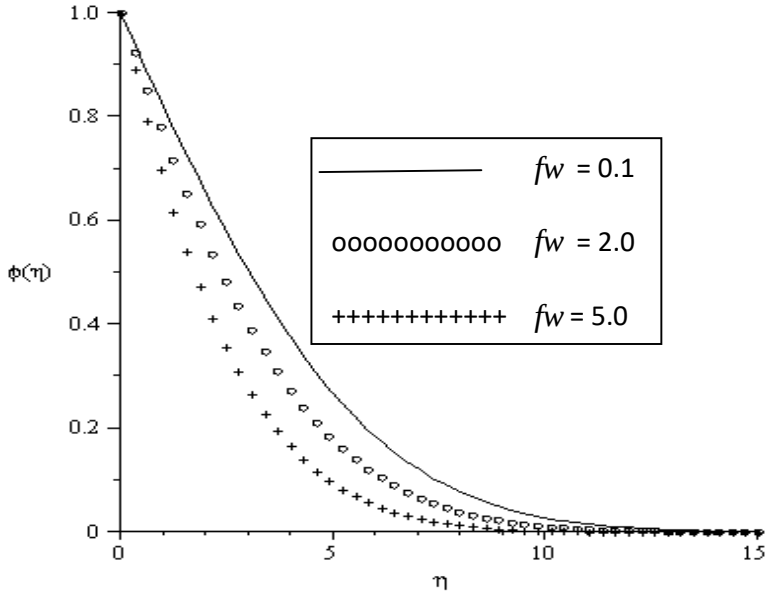

Figure 16: Concentration distribution for various values of suction parameter fw for various values of **Gr= Ra = Ec= Gc = Bi = Sc = 0.1. Pr = 0.1,** β **= 0.1,** λ **= 0.1**

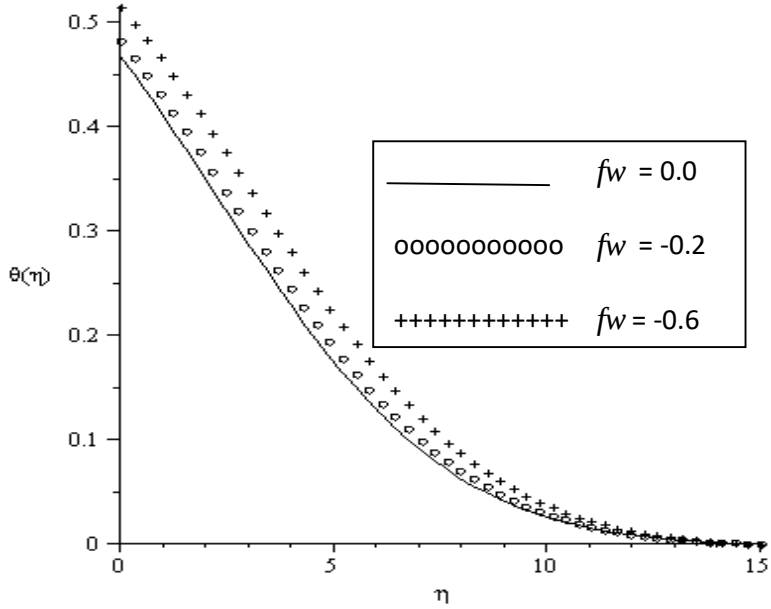

Figure 17: Temperature distribution for various values of suction parameter fw for various values of **Gr= Ra = Ec= Gc = Bi = Sc = 0.1. Pr = 0.1,** β **= 0.1,** λ **= 0.1**

4.0 CONCLUSION

It was observed that when the Solutal Grashof number Gc, thermal radiation parameter Ra and the internal heat generation parameter β increases, the Skin-friction coefficient and heat transfer rate increases while the mass transfer rate increases. It was also noticed that when the Schmitt number Sc and the chemical reaction parameter λ increases, the Skin-friction coefficient, heat transfer rate and the mass transfer rate at the wall increases. It implies that the Schmitz number and the chemical reaction parameters enhance the skin-friction coefficient, mass transfer rate and the heat transfer rate at the wall surface. We also observed that as the suction parameter fw, Eckert number Ec and the Biot number Bi increases, the skin-friction coefficient decreases while the heat and mass transfer rate at the wall decreases. Finally, as the injection parameter fw <0 increases, the skin-friction coefficient increases while the heat and mass transfer rate at the wall surface decreases. It is also noticed that injection increases the fluid flow while suction reduces the fluid flow velocity.

REFERENCES

Abdelraheem, MA, Sameh, EA, Raizah, ZAS (2018). Double-diffusive natural convection in a square porous cavity with sinusoidal distributions side walls filled with a nanofluid, Journal of porous media, 2. 101-122.

Akbar, N., Khan, Z., Nadeem, S., & Khan, W. (2016). Double-diffusive natural convective boundary layer flow of a nano fluid over a stretching sheet with magnetic field . International journal of numerical methods for heat and fluid flow, 26, (1), 108-121.

Baiyeri, JF, Esan, OA, Ogunbayo, TO, Enobabor, OE, Salawu, SO (2017). Analysis of unsteady hydromagnetic natural convective dissipative flow through an inclined plate. Asian Journal of Physical and Chemical Sciences, 2(2), 1-12.

Bejan, A. Dincer, I. Lorente, SA, Miguel, AF, Reis AH, (2004). Porous and complex flow structures in modern technologies, Springer, New York.

Cheng, CY (2009). Non-similar boundary layer analysis of double-diffusive convection from a vertical truncated can in a porous medium with variable viscosity. Applied Math. Comput. 212, 187-193.

Dada, MS, Salawu SO (2017). Analysis of heat and mass Transfer of an inclined magnetic field **p**ressure-driven flow past a permeable Plate. Applications and Applied mathematics: An International Journal, 12(1); 189 – 200

Gaikwad, SN, Kamble, SS (2016). Cross diffusion effects on the set of double diffusive convection in a couple stress fluid saturated rotating anisotropic porous layer. Journal of applied mechanics 9; 4, 1645-1654.

Incropera, FP, Dewitt, DP, Bergman, TL, Lavine, AS (2007). Fundamentals of heat and mass Transfer, 6th edition John Wiley, New York.

Ingham, D.B. Pop, I. (2002). Transport phenomena in porous media, vol. III, Elsevier, Oxford.

Ishak, A (2010) Similarity solutions for flow and heat transfer over a permeable surface with convective boundary condition. Appl Math Comput. 217:837–842.

Kareem, A, Salawu, S (2017). Variable viscosity and thermal conductivity effect of soret and dufour on inclined magnetic field in non-Darcy permeable medium with dissipation. British Journal of Mathematics & Computer Science, 22(3), 1-12.

Mohamad, A (2004). Double diffusion natural convection in a rectangular enclosure filled with binary fluid saturated porous media: The effect of lateral aspect ratio, Physics of Fluids 16, 184.

Mohamed RA, (2009). Double-diffusive convection radiation interaction on unsteady MHD flow over a vertical moving porous plate with heat generation and soret effect. Appl math sci. 3:629-51.

Okedoye, AM, Salawu**,** SO (2019). Unsteady oscillatory MHD boundary layer flow past a moving plate with mass transfer and binary chemical reaction. SN Applied Sciences, 1(9), 1586.

Olanrewaju, PO, Alao, FI, Adeniyan, A, Bishop, SA (2013). Double-diffusive convection from a permeable vertical surface under convective boundary condition in the presence of heat generation and thermal radiation, Nonlinear Sci. Lett. A, 4(3), 76-90.

Olanrewaju PO, Gbadeyan JA, Hayat T, Hendi AA. (2011) Effects of internal heat generation, thermal radiation and buoyancy force on a boundary layer over a vertical plate with a convective surface boundary condition. S Afr J Sci. 107(9/10), 476-482.

Salawu, S., & Kareem, A. (2019). Analysis of heat absorption viscoelastic exothermic chemical reactive fluid with temperature dependent viscosity under bimolecular kinetic. Applications and Applied Mathematics: An International Journal, 14(2); 1232 – 1242.

Salawu, SO, Amoo, SA (2016). Magnetohydrodynamics effects on radiative and dissipative heat transfer near a stagnation point with variable viscosity and thermal conductivity. Computing, Information Systems, Development Informatics and Allied Research Journal, 7(4), 51-62.

Salawu, SO, Amoo, SA (2016). Effects of variable viscosity and thermal conductivity on dissipative heat and mass transfer of MHD flow in a porous medium. AIMS Research Journal, 2(2), 111-122.

Subhashini SV, Samuel N, Pop I (2011). Double-diffusive convection from a permeable vertical surface under convective boundary condition, International Communications in Heat and Mass Transfer 38: 1183–1188.

Yadav, D, Agrawal, S. (2013), on set of double-diffusive nano-fluid convection in a layer of thermal conductivity and viscosity variation. Journal of porous media 16; 2, 105-121.

Yang, Z, Wang, S, Zhao, M, Li, S, Zhang, Q (2013). The Onset of double diffusive convection in a viscoelastic fluid-saturated porous layer with non-equilibrium model. PLoS ONE 8(11): e79956.

ANTIMICROBIAL AND PHYTOCHEMICAL POTENTIALS OF METHANOLIC EXTRACT OF MOMORDICA CHARANTIA (LINN) LEAVES AGAINST SOME BACTERIA AND FUNGI

Kolawole-Joseph, O. S[1]., **Amolegbe,** O.A[1]., **Rufai,** O. K[2]., **Ajayi,** J.B[3]., and [1]**Kolade, T.T.**

[1]Department of Biological Science, Yaba College of Technology, Yaba Lagos.
[2]Ogun State College of Health Technology, Department of Emergency Medical Technology, Ilese Ijebu, Ogun state.
3 Ogun State Institute of Technology, Microbioology Unit, Department of Science Laboratory Technology, Igbesa, Ogun State

Corresponding author: *Kolawolejoseph2006@yahoo.com*

ABSTRACT

Momordica charantia is a plant used traditionally for the treatment of infectious diseases. Antimicrobial and phytochemicals potential of methanolic extract of *M. charantia* on six bacteria and five fungi was investigated in this study. The leaves were collected, washed, air-dried and ground. 300g ground powder was soaked in 1200mls of methanol and extracted over a seven day period, filtered and the extract was evaporated to dryness and stored in screw capped bottles. The antibacterial and antifungal potentials was investigated using agar-well diffusion methods while phytochemical screening was investigated using standard procedure. Result of the phytochemical screening revealed the presence of alkaloids (12.40µg/mL), saponins (10.45µg/mL), terpenoids (12.20µg/mL), flavonoids (09.20µg/mL), cardiac glycoside (16.80µg/mL) and phenol (02.40µg/mL). Cardiac glycoside had the highest concentration while phenol had the lowest concentration. The antibacterial result showed concentration of 600µg/mL and 300µg/mL inhibited the growth of the tested bacteria except *Klebsiella* oxytoca which had no inhibition. *Staphylococcus aureus* was most active while *Staphylococcus epidermidis* was least active. Streptomycin used as positive control was effective against all the bacteria except *Klebsiella oxytoca*. The diameter of zones of inhibition ranged from 20.67mm and 12.50mm with *Staphylococcus aureus* having the highest zone of inhibition while *K. oxytoca* had no inhibition. The antifungal result showed that *Fusarium* sp had the highest zone of inhibition of 10.20mm while *Candida albicans* had the lowest inhibition of 02.50µg/mL and *Aspergillus niger* had no inhibition. Funamycin used as positive control was effective against all the fungi. The results obtained in this study reveal that the use of *M. charantia* in herbal medicine could be used as a source of oral antimicrobial agent for the treatment of diseases associated with these microorganisms.

KEYWORDS:
Activity, bacteria, fungi, phytochemical, plants

INTRODUCTION

Medicinal plants are considerably useful and contain active constituents that are economically essential. They contain active constituents that are used in the treatment of some human diseases. Plant extracts have been developed and proposed for use as antimicrobial substances. All parts of *M. charantia* including the fruit taste bitter (Khan *et al.* 2019). Indigenous plants are the first source of therapy for most of the common ailments in developing countries like Nigeria because of its availability, economic status of the users and incidence of resistant or multi resistant strains (Sofowora, 2013). Plants derived drugs is mainly due to the current widespread belief that green medicine is safer and more dependable than costly synthetic drugs which have many side effects (Sumathi and Parvatti, 2010). Plants have naturally occurring chemicals that are non-nutritive but are for their self-protection. The plant act as a source of carbohydrate, proteins, minerals, vitamins and other nutrients for human to maintain health (Ullar *et al.*, 2018). *Momordica charantia* is commonly known as

bitter melon or bitter gourd. It is an economically important, successful medicinal and vegetable plant for human health and belonging to the family Cucurbitaceae (Khan *et al.* 2019). In Nigeria, it is called by local names which include: Ejirin (Yoruba), Daladdasu (Hausa) and Okwunuolo (Igbo). It is widely grown in Asia, Africa and the Caribbean. The fruit juice or leaf tea is employed in the treatment of diabetes, malaria, colic, sores and wounds infections, measles, hepatitis and fevers. Leaves are used for treating catarrh, constipation, dermatitis, dysentery, diarrhea, eczema, fever, leprosy, snake bite, anaemia. (Kandangath *et al*., 2015: Snee *et al*., 2011). Young Momordica shoots and leaves are also cooked and eaten as leafy vegetables. Leaf and fruit extracts are used in the preparation of tea (Kandangath *et al*., 2015). The textured leaves look like a bite that is why the plant is given the name Momordica which means to bite (Prarthna *et al*., 2014). *M. charantia* is known to be a powerful nutrient dense plant composed of a complex array of beneficial compounds (Bakare *et al*. 2014). Medicinal value of bitter melon has been attributed to its high antioxidant properties due in parts of phenols, flavonoids, isoflavones, alkaloids; glycoside, saponin and tannin (Snee *et al*., 2011). *M. charantia* fruit and leaves contain alkaloids, glycoside, saponin like substances, rennin and aromatic volatile oil mucilage (Leelaprakash *et al*., 2011). Extracts of *M. charantia* had antimicrobial effects against *Staphylococcus aureus, Pseudomonas aeruginosa, Candida epicola, Candida albicans, Candida tropicalis* and *Penicillium* sp (Akanji *et al*., 2016; Mahmood *et al*., 2012; Shuo *et al*., 2017). It is therefore essential to examine plants of medicinal value for their promising biological activity (Sofowora, 2013). Virtually all plants are medicinal; hence they serve as raw materials for synthetic drugs. Sofowora *et al.* (2013) noted that the medicinal value of these plants lies in the bioactive phytochemical constituents that produce definite physiological action on the human body. Ethanol extract of bitter melon leaves are considered to have an antibacterial action against *Salmonella, Pseudomonas aeruginosa, Escherichia coli, Bacillus* and *Streptococcus* species (Brandao *et al*. 2016; Paul *et al*., 2010; Leelaprakash *et al*., 2011). People in the rural areas where modern medical facilities cannot satisfy their medical demands are mostly affected as about 80% of these people rely on traditional medicine (Teoh *et al*., 2010). It is therefore imperative to investigate the efficacy of *Momordica charantia* against some bacteria and fungi as claimed by local traditional herbalists.

2.0 MATERIALS AND METHODS

2.1 Plant Collection, Extraction and Concentration

The leaves of *Momordica charantia* were collected in the wild at 'Ogolonto' bus stop with latitude: 6.6000 and Longitude: 3,5000 along Ikorodu road, Lagos. The plant parts were identified at the herbarium unit of Plant Science Department of Olabisi Onabanjo University, Ago-iwoye Ogun State, Nigeria. The plants were properly washed and drained. After washing, the plants were dried for 21 days under room temperature ($28^{O}C \pm 2$). The leaves of *M. charantia* were pulverized after drying. 300g of ground *M. charantia* was weighed and soaked in 1200mL of methanol for 7 days. After soaking, the mixture was pre-filtered using muslin cloth and No1 Whatman's filter paper and then stored in a screwed cap bottle (Mada *et al*., 2013).The filtrate were then separately concentrated in vacuo using Rotary Evaporator (Model E52A, China) to 10% of their original volume at $40^{0}C$. These were concentrated to complete dryness in water bath. The reconstituted extract were transferred to the Biochemistry Laboratory and Pharmaceutical Microbiology Research Laboratory, College of Medicine, Idi-araba Lagos for Phytochemical screening and Antimicrobial Susceptibility testing.

2.2 Preparation of stock solutions and concentrates

The stock solutions of the bacteria and fungi were obtained at the Pharmaceutical Microbiology Research Laboratory, College

of Medicine, Idi-araba Lagos and were prepared as described in the CLSI guidelines (M07-A6, 2003) for bacteria. Stock solutions of Streptomycin and Funamycin (positive controls) were diluted in 5 % DMSO (dimethyl sulphoxide) at a density adjusted to a 0.5 McFarland turbidity standard 10^5colony-forming units (CFU)/ml for bacterial cultures. The plant extracts were dissolved in 5 % DMSO to obtain a final concentration of 600, 300, 150µg/mL.

2.3 In vitro Screening of Antimicrobial Activity of *M. charantia*

Mueller-Hinton Agar were used for the antimicrobial sensitivity screening. Potatoe Dextrose Agar plates were used for the antifungal sensitivity screening. The plates were seeded with the bacterial cells and fungal cells and allowed to stand for 1h in the lamina air-flow hood for the test bacterial isolates and fungal isolates to be fully embedded and well established in the seeded medium. With a sterile No. 4 cork borer, wells of 5mm diameter were dug with a previously sterilized No 4 cork borer. The wells were aseptically filled up with 0.1mL of *M. charantia* methanolic extract avoiding splash and overfilling. Duplicates plates were also prepared for the bacterial and fungal isolates. The plates were incubated at 37^0C for 24-48 h for bacteria and 25^0C for fungi. The sensitivity of the test organisms on the extract were indicated by clear halo around the wells on the bacterial and fungal plates. The halo diameters were taken as an index of the degree of sensitivity for both bacterial and fungal plates. The bacteria and fungi used are *as* follows: *Escherichia coli, Staphylococcus aureus, Bacillus subtilis, Klebsiella oxytoca, Staphylococcus epidermidis, Pseudomonas aeruginosa* and *Penicillium* sp, *Fusarium* sp, *Aspergillus niger, Candida albicans* and *Aspergillus flavus.*

2.4 Minimum Inhibitory Concentration (MIC) of methanolic extract *M. charantia*

The Minimum inhibitory concentration (MIC) of the plant extracts on the test bacterial isolates were determined by the agar micro dilution method as described by the CLSI guidelines (M07-A6, 2003) for bacteria. The stock solutions were further diluted in a 2-fold serial dilution to obtain the following concentrations: 600, 300 and 150µg/mL. Agar plates were prepared by pouring MHA for bacterial isolates into sterile Petri plates containing 1ml of the various dilutions of the extract. The test isolates which were grown overnight in nutrient broth were adjusted to McFarland 0.5 standard and streaked onto the surface of the agar plates containing dilutions of the plant extract. The MHA plates were then incubated at 37°C for 24 hours after which all plates were observed for growth. The minimum dilution (concentration) of the extracts completely inhibiting the growth of each organism was taken as the MIC.

2.5 Minimum Fungicidal Concentration (MFC) of *M. charantia*

The methods adopted for antibacterial activity was also adopted for the Minimum Fungicidal Concentration using *Penicillium* sp, *Fusarium* sp, *Aspergillus niger, Candida albicans* and *Aspergillus flavus* and the plates were incubated at 25^0C for 24-48hrs

.

2.6 Qualitative and Quantitative Phytochemical Screening of *M. charantia*

Qualitative and Quantitative Phytochemical analysis of *M. charantia* were performed using the methods described by Edeoga *et al.* (2021) and were screened for the presence of the following phytochemicals: Alkaloids, Saponin, Terpenoid, Flavonoid, Cardiac glycoside and Phenol using methanol as solvent.

3.0 RESULTS

Table 1 shows the result of the antibacterial assay of *M. charantia* at various concentrations of 600, 300 and 150 ug/mL. *M. charantia* showed activity ranging from 20.67-12 and *Klebsiella oxytoca* had no activity in all the concentrations. Streptomycin positive control used was effective against *Pseudomonas aeruginosa, Staphylococcus aureus, Bacillus subtilis* and *Staphylococcus epidermidis* but inactive against *Klebsiella oxytoca.*

Table 1: Antibacterial Activity of methanolic extract of *M. charantia*

Concentration (µg/mL**)**	**Bacterial strain**	**Plant zones of inhibition (mm)**	**Streptomycin(mm)**
600µg/mL	*Escherichia coli*	17.00	09.00
	Pseudomonas aeruginosa	14.00	06.00
	Staphylococcus aureus	20.67	12.00
	Bacillus subtilis	18.50	08.00
	Klebsiella oxytoca	0.00	0.00
	Staphylococcus epidermidis	12.50	07.00
300µg/mL	*Escherichia coli*	15.00	06.00
	Pseudomonas aeruginosa	12.00	05.00
	Staphylococcus aureus	14.67	08.00
	Bacillus subtilis	14.00	0.400
	Klebsiella oxytoca	0.00	0.00
	Staphylococcus epidermidis	10.50	04.00
150µg/mL	*Escherichia coli*	06.00	02.00
	Pseudomonas aeruginosa	04.20	03.00
	Staphylococcus aureus	07.00	04.00
	Bacillus subtilis	05.50	02.00
	Klebsiella oxytoca	0.00	0.00
	Staphylococcus epidermidis	03.50	03.00

Table 2 shows the result of the antifungal assay of *M. charantia* at various concentrations of 600, 300 and 150ug/mL *M. charantia* showed antifungal activity ranging from 10.20-02.50mm and *Aspergillus* sp had no activity and these values do not differ significantly from each other ($p < 0.05$). Funamycin used as positive control was effective against *Penicillium* sp, *Fusarium* sp, *Apergillus niger, Candida albicans* and *Aspergillus flavus.*

Table 2: Antifungal Activity of methanolic extract of *M. charantia*

Concentration (µg/mL**)**	**Fungal strains**	**Plant zones of inhibition (mm)**	**Funamycin**
600µg/mL	*Penicillium* sp	08.00	06.00
	Fusarium sp	10.20	08.00
	Apergillus niger	08.00	04.00
	Candida albicans	02.50	03.00
	Aspergillus flavus	0.00	02.00
300µg/mL	*Penicillium* sp	04.00	04.00
	Fusarium sp	03.20	05.00
	Apergillus niger	01.00	02.00
	Candida albicans	01.50	02.00
	Aspergillus flavus	0.00	01.00
150µg/mL	*Penicillium* sp	02.00	02.00

	Fusarium sp	02.20	03.00
	Apergillus niger	03.00	01.00
	Candida albicans	02.50	01.00
	Aspergillus flavus	0.00	01.00

Table 3 shows the result of *M. charantia* MIC against the bacterial isolates which ranged from 62.5-07.08mm, *M. charantia. Staphylococcus aureus* had the highest MIC while *Klebsiella oxytoca* had the lowest.

Table 3: Minimum Inhibitory Concentration MIC) of methanolic extract of *M. charantia* against some selected bacteria

Bacterial strains	**MIC (**µg/mL**) Results**
Escherichia coli	31.3
Pseudomonas aeruginosa	15.7
Staphylococcus aureus	62.5
Bacillus subtilis	31.3
Klebsiella oxytoca	00.0
Staphylococcus epidermidis	15.7

Table 4 show that the result of the phytochemical (qualitative) analysis of crude methanolic extract of *M. charantia* revealed the presence of Alkaloids (12.50 µg/mL), saponin (10.45 µg/mL), terpenoid (12.20 µg/mL), flavonoid (09.20 µg/mL), cardiac glycoside (16.80 µg/mL) and phenol (02.40 µg/mL). Cardiac glycoside was the highest while phenol had the least value.

Table 4. Qualitative and quantitative Phytochemical analysis of ethanol extract of *M. charantia*

Bioactive compounds	**Qualitative result**	**Quantitative Results (µg/mL)**
Alkaloid	Positive	12.50±0.1
Saponin	Positive	10.45±0.2
Terpenoid	Positive	12.20±0.2
Flavonoid	Positive	09.20±0.1
Cardiac glycoside	Positive	16.80±0.1
Phenol	Positive	02.40±0.2

4.0 DISCUSSION

The antimicrobial activity results show that methanolic extract of *M. charantia* was effective against *Escherichia coli, Pseudomonas aeruginosa, Staphylococcus aureus, Bacillus subtilis* and *Staphylococcus epidermidis. Staphylococcus aureus* had the highest activity while *Staphylococcus epidermidis* had the lowest while *Klebsiella oxytoca* had no activity at the various concentrations. Streptomycin used as the positive control was effective against all the bacteria except *Klebsiella oxytoca*. The antifungal susceptibility testing showed high activity against *Fusarium* sp while *Candida albicans* had the lowest activity and *Aspergillus niger* had no activity at the various concentrations. Funamycin used as the positive control was effective against all the fungi. This result also agrees with the findings of Mahmood *et al*. (2012); Akanji *et al*. (2016); Shuo *et al.* (2017) in a study of the **antimicrobial activity** of crude methanolic, leaf extracts of, *M. charantia.* Extracts of *M. charantia* showed positive **antibacterial activity,** having the highest inhibitory action on the bacterial isolates except *Klebsiella oxytoca*. Extracts of *M. charantia* showed broad spectrum **antifungal activity,** having the highest inhibitory action on the fungal isolates except *Aspergillus niger*. The effectiveness of these plant extracts against some pathogenic bacteria species was also evident in the minimum inhibitory concentrations recorded. The minimum inhibitory concentration (MIC) ranged from 62.5-07.08µg/mL. The result of the phytochemical screening of *M. charantia* revealed the presence of alkaloids, terpenoid, flavonoid, cardiac glycoside and phenol. This result agrees with the findings of Snee *et al.*(2011); Aparna *et al*. (2015) who found alkaloids, glycosides, saponin, and rennin in methanolic extracts of *M. charantia.* A study conducted by Leelaprakash *et al.* (2011)

revealed the presence of alkaloids, flavonoids, tannins, phenols, glycosides and saponins on *M. charantia.* The roles of these phytochemicals in plants have been well documented. According to Hasler and Blumberg (2017), phytochemicals are biologically active, naturally occurring chemical compounds found in plants which provide health benefits for humans further than those attributed to macronutrients and micronutrients. The phenols have been reported to possess considerable antimicrobial properties attributed to their redox properties (Eleazu *et al.,* 2012. In addition, flavonoids have also been reported to possess antimicrobial and anti-inflammatory properties. Khan *et al.* (2011) also reported that alkaloids and flavonoids are responsible for the antifungal activities in higher plants. Some of the characteristics of saponins include formation of foams in aqueous solutions, haemolytic activity and cholesterol-binding properties (Eleazu *et al.,* 2012). *M. charantia* contain an array of bioactive compounds and may be used to treat some bacterial and fungal infections.

4.1 CONCLUSION

Results of this study therefore suggest that methanolic extract of the leaves of *M. charantia* contain a wide array of bioactive phytochemical constituents regardless of the seasons they were obtained, and are potential antibacterial and antifungal properties equally safe for consumption to treat some diseases associated with these bacteria and fungi used in this study.

ACKNOWLEDGEMENT

We acknowledge Professor N.A. Amusa, of Department of Microbiology, Western Union University, Okun-Owa Ogun State. Staff of Microbiology laboratory, Yaba College of Technology. Staff of pharmaceutical microbiology research laboratory, College of Medicine, Universitv of Lagos and staff of Plant Science department, Olabisi Onabanjo University, Ago-Iwoye, Ogun state for their contributions towards the success of this research.

REFERENCES

Akanji, O. C., Cyril, C. M., Eluhoye, O. I. and Ogunsun, O. O. (2016). The Antimalaria Effect of *Momordica charantia* L. and *Mirabilis jalapa* Leaf Extracts Using Animals Model. *Journal of Medicinal Plants Research*, 10(24): 344-350.

Akinmoladun, A.C., Obuotor, E.M. and Farombi, E.O. (2010). Evaluation of Antioxidant and Free Radical Scavenging Capacities of Some Nigerian Indigenous Medicinal Plants. *Journal of Medicinal food.* (2)13: 0292-1089.

Bakare, R.I., Magbagbeola, O.A., Akinwande, A.I. and Okunowo, O.W. (2014). Nutritional and Chemical evaluation of *Mormodica charantia*. *Journal of Medical Plant Research*, 4 (21): 2189-2193.

Brandao, T., Tavares, R., Schulz, M.S. and Matos, P.M. (2016). Measuring Emotion Regulation and Emotional Expression in Breast Cancer Patients: *A Systematic Review*. *Clinical Psychology Review* 43: 114-127.

Clinical and Laboratory Standard Institute (CLSI) (2003). Methods for dilution antimicrobial susceptibility tests for bacteria that grow aerobically. Wayne, PA: CLSI; [*document MO7-A6*].

Edeoga, H.O., Okwu, D.E., Mbaebie, and B.O. (2021). Phytochemical Constituents of Some Nigerian Medicinal Plants. *African Journal of Biotechnology*. 4(7): 685-688.

Eleazu, C.O., Eleazu, K.C. Awa, E. and Chukwuma, S.C. (2012). Comparative Study of The Phytochemical Composition of The Leaves of Five Nigerian Medicinal Plants. *Journal of Biotechnology and Pharmaceutical Research*. 3(2): 42-46.

Hasler, C.M. and Blumberg, J.B. (2017). Analysis of Bioactive Compounds and Elemental Analysis in *Eichhoria grassipes* leaf. *World Journal of Pharmaceutical Research.* 16(6):1083-1092.

Kandangath, A.K. and Xiaoyuan, T.U. (2015). Humanized Navigation Iinstructions for Mapping Applications. *US Patient Applications*. 14. 176-455.

Khan, N. H., Amy, Linn, A.T.S. and Perveen, N. (2019). Phytochemical Analysis, Antibacterial and Antioxidant Activity Determination of *Momordica charantia*. *World Journal of Pharmacy and Pharmaceutical Sciences*. 2(8):81-96.

Leelaprakash, G., Rose, J.C., Growtham, B.M., Javvaji, P.K. and Prasa, S.A. (2011). In-vitro Antimicrobial and Antioxidant Activity of *Momordicacharantia* Leaves. *Pharmacophore*, 2(4): 244-252.

Mahmood, A., Raja, G.K., Mahmood, T., Gulfraz, M. and Khanum A. (2012). Isolation and Characterization of Antimicrobial Activity Conferring Components from Seeds of Bitter Gourd (*Momordica charantia*). *Journal of Medicinal Plants Research.* 6(4):566-573.

Mada, S.M., Garba, H.A., Muhammad, A., Olagunju, A. and Muhammad, A.B. (2013). Antimicrobial Activity and Phytochemical Screening of Aqueous and Ethanol Extracts of *M. charantia* L. leaves. *Journal of Medicinal Plants research*. 7(10): 579-586.

Prarthna, D., Ujjwala, S. and Roymon, M.G. (2014). A Review on Phytochemical Analysis of *Momordica charantia. International Journal of Advances in Pharmacy, Biology and Chemistry.* 3(1):214-220.

Shuo, J., Mingyue, S., Fan, Z. and Jianhua, X. (2017). Recent Advances in *Momordica charantia*: Functional Components and Biological Activities. *International Journal of Molecular Sciences.*12(18): 2555.

Snee, L. S., Nerurkar, V. R., Deoley, D. A., Efird, J. T., Shovic, A. C. and Nerurkar, P. V. (2011). Strategies to Improve Palatability and Increase Consumption Intentions of *Momordica charantia* (Bitter Mmelon). A Vegetable Commonly Used for Diabetes Management *Nutritional Journal.* 10(1):78.

Sofowora, A., Ogunbodede, E. and Onayade, O. (2013). The Role and Play of Medicinal Plants in The Strategies for Disease Prevention. *African Journal of Traditional Complementary and Alternative Medicines.*10(5): 210-229 2: 213-221

Sumathi, P. and Parvathi, A. (2010). Antimicrobial Activity of Some Traditional Medicinal Plants. *Journal of Medicinal Plants Research.* 4, 316-321

Ullar, I., Ali, N.and Durrani, A.W. (2018). Effect of Different Nitrogen Levels on Growth, Yield and Yield Contributing Attributes of Wheat. *International Journal of Scientific and Engineering.* 9(9):1SSN 2229-5518

Ulla, M, Chy, F.K., Sarkar, S.K., Islam, M.K. and Absar, N. (2011). Nutient and Phytochemical Analysis of Four Varieties of Bitter Gourd (*Momordica charantia*) Grown in Chitagong Hill Tracts, Bangladesh. *Asian Journal of Agricultural Research*. 3(5):186-193)

INTERNATIONAL, JOURNAL OF SCIENCE & SOCIETY YABATECH
VOL 7, No 1, JUNE 2021. ISSN: 2276-7924

ANTIMICROBIAL AND PHYTOCHEMICAL POTENTIALS OF PHYSALIS ANGULATA L. LEAVES AGAINST SOME BACTERIA AND FUNGI

Kolawole-Joseph, O. S.[1], **Amolegbe,** O.A.[1], **Rufai,** O. K[2]., **Ajayi,** J.B.[3] and [1]**Kolade,** T.T.

[1]Department of Biological Science, Yaba College of Technology, Yaba Lagos.
[2]Ogun State College of Health Technology, Department of Emergency Medical Technology, Ilese Ijebu, Ogun state.
[3]Ogun State Institute of Technology, Microbioology Unit, Department of Science Laboratory Technology, Igbesa, Ogun State

Corresponding author: *Kolawolejoseph2006@yahoo.com*

ABSTRACT

Physalis angulata belong to the family Solanaceae. Plants have the ability to synthesise a wide variety of chemical compounds that are used to perform important biological functions. In this study we aim at investigating the antimicrobial activity and phytochemical potential of methanolic extract of the leaves of *Physalis angulata* on some bacteria and fungi. *P. angulata.* leaves were collected, washed, air-dried and ground. 300g of the ground powder was soaked in 1200 mls of methanol and extracted, filtered. The crude extract was evaporated to dryness and stored in a screw capped bottle. The antibacterial and antifungal potentials of the plant extract was investigated using agar-well diffusion methods while phytochemical screening was investigated using standard procedure. The antibacterial result showed that a concentration of 600 µg/mL, 300 µg/mL and 150 µg/mL inhibited the growth of the tested bacteria and fungi. *Bacillus subtilis* was the most effective while *Klebsiella oxytoca* was the least effective. The diameter of zones of inhibition obtained ranged from 15.50mm and 05.40mm. Streptomycin used as the positive control was effective against all the bacteria. The antifungal result showed that *Aspergillus niger* had the highest zone of inhibition of 06.00mm while *Fusarium* sp had the lowest inhibition of 02.00mm while *Penicillium* sp. and *Candida albicans* had no inhibition at all. Funamycin used as the positive control was effective against *Fusariun* sp, *Aspergillus niger* and *Aspergillus flavus* while there was no inhibition in *Penicillium* sp, and *Candida albicans*. Phytochemical screening result revealed the presence of alkaloids (08.70µg/mL), saponins (10.30µg/mL), terpenoids (09.50µg/mL), flavonoids (10.40µg/mL), cardiac glycoside (14.40µg/mL) and phenol (07.50 µg/mL). Cardiac glycoside had the highest concentration while phenol had the lowest concentration. The results obtained in this study revealed that *P. angulata* in herbal medicine could be used as a source of oral antimicrobial agent for the treatment of diseases associated with these microorganisms.

KEYWORDS:
Activity, bacteria, fungi, phytochemical, plants

1.0 INTRODUCTION

Plants and herbs are used in the preparation of medicines and treatment of various diseases from the ancient time. Over the past two decades there is increase in the use of herbal medicine. About 70-80% of world population uses the plants derived traditional methods for the treatment of various health problems. The availability of medicinal plants and their cheaper cost to modern therapeutic agents makes them more attractive as therapeutic agents (Soladoye *et al.,* 2014). Plants have naturally occurring chemicals that are non-nutritive and for their self-protection. Today the use of plant material as functional foods and nutraceutical for the treatment of different diseases is on the increase all over the world. These could be linked to their phytochemical constituents which include phenolic acids, flavonoids and alkaloids. These

phytochemicals have several health benefits with little or no side effects compared to synthetic product. *Physalis* is a genus of flowering plants in the nightshade family of Solanaceae, which grow in warm weather condition. The family has a wide global distribution with about 75-90 known species of the genus Physalis. (Kumar *et al.,* 2016). *Physalis angulata* is known by different names including; cutleaf ground cherry, wild tomato, mullaca, winter cherry. In south west Nigeria, it is commonly known as "koropo" (Osho *et al.,* 2010). The plant is of high economically importance because of its medicinal properties, used as the whole plant as well as parts of the plant. The extract of *Physalis* exhibits in vitro antimicrobial action against some bacterial and fungal pathogenic organisms. (Kumar *et al.,* 2016). Organic extracts of the whole plant exhibit immunomodulatory, Anti-inflammatory, anticancer, antinociceptive, trypanocidal, antimicrobial, molluscidal, Antigonorrheal and Antioxidant effects (Sandhya *et al.,* 2010). The juice is used in the treatment of ear-ache, jaundice, fever, bladder disease. The fruit and other aerial parts are used for the treatment of boils, sores, cuts, constipation, intestinal and digestive problems. It is also used in the treatment of hepatitis, diabetes, asthma, and malaria (Osho *et al.,* 2010). Osho *et al.* (2010) in his findings on antimicrobial activity of essential oil of *P. angulata* at different concentration by agar well diffusion method reported that *P. aeruginosa* was resistant to the essential oil from both the aerial and root part of the plant. The minimum inhibitory concentrations (MIC) which ranged between 3.75 mg/ml and 4.0mg/ml were recorded for *Bacillus subtilis, Klebsiella pneumoniae* by the aerial and root extracts, but *P. aeruginosa* and *S. aureus* were not susceptible to the aerial and root extract. *P. angulata* oil extract has antibacterial properties, and it is a promising antimicrobial agent which is important for the treatment of sores, cut, intestinal and digestive problem and some skin disease (Osho *et al.,* 2010). Donkor *et al.* (2012) in his study on the inhibitory activity of zinc oxide-ointment formulations as well as the unformulated crude extract of fruits of *P. angulata* investigated against clinical wound isolates of *S. aureus* and *P. aeruginosa* and were found to be effective against *S. aureus* in all the concentrations used. Previous researchers had focused on isolation and characterization of secondary metabolites and demonstrated that some of the extracts or active principles obtained from Physalin species have a broad spectrum of biological activities which includes antitumor, antibacterial, antifungal (Damu *et al*. (2007). It was also reported by Silva *et al*. (2005) that the crude extract from *P. angulate* aerial parts contain antibacterial and phytochemical constituents. Ushie *et al*. (2019) reported in his study on phytochemical screening and antimicrobial activities of Chloroform and Ethyl Acetate Extract of *P. angulata* that the detection of some phytochemicals is an indication that *Physalis angulata* can be seen as a potential source of useful drugs preparation.

2.0 MATERIALS AND METHODS

2.1 Plant Extraction (Maceration) and concentration

The leaves of *P. angulata* were collected at 'Ogolonto' bus stop with latitude: 6.6000 and Longitude: 3, 5000 along Ikorodu road, Lagos. The plant parts were identified at the herbarium unit of Plant Science Department of Olabisi Onabanjo University, Ago-iwoye Ogun State, Nigeria. The plants were properly washed and drained. After washing, the plants were dried for 21 days under room temperature ($28^{O}C$ ±2). The leaves of *P. angulata* were pulverized after drying. 300g of ground *P. angulata* was weighed and soaked in 1200ml of methanol for 7 days. After soaking, the mixture was pre-filtered using muslin cloth and then with No1 Whatman's filter paper and then stored in a screwed cap bottle (Mada *et al*., 2013). The filtrate were then separately concentrated in vacuo using Rotary Evaporator (Model E52A, China) to 10% of their original volume at $40^{0}C$. These were concentrated to complete dryness in water bath.

2.2 Preparation of stock solutions and concentrates

Stock solutions of the stock cultures were prepared as described in the CLSI guidelines (M07-A6, 2003) for bacteria. Stock solutions of Streptomycin and Funamycin (positive controls) were diluted in 5 % Dimethyl sulphoxide (DMSO) at a density adjusted to a 0.5 McFarland turbidity standard 10^5colony-forming units (CFU)/ml for bacterial cultures, while methanol used as negative control was diluted with 2% sterile water. The plant extracts were dissolved in 5 % DMSO to obtain a final concentration of 600, 300, 150 µg/ml.

2.3 In vitro Screening of Antimicrobial Activity of *P. angulata* methanolic leaves extract

Mueller-Hinton Agar (MHA) were used for the antimicrobial sensitivity screening. Potatoe Dextrose Agar plates were used for the antifungal sensitivity screening. The plates were seeded with the bacterial cells and fungal cells and allowed to stand for 1h in the lamina air-flow hood for the test bacterial isolates and fungal isolates to be fully embedded and well established in the seeded medium. With a sterile No. 4 cork borer, wells of 5mm diameter were dug with a previously sterilized No 4 cork borer. The wells were aseptically filled up with 0.1mL of *P. angulata* methanolic extract avoiding splash and overfilling. Duplicates plates were also prepared for the bacterial and fungal isolates. The plates were incubated at 37^0C for 24-48 h for bacteria and 25^0C for fungi. The sensitivity of the test organisms to each of the extracts were indicated by clear halo around the wells on the plates. The halo diameters were taken as an index of the degree of sensitivity. The bacteria and fungi used are *as* follows: *Escherichia coli, Staphylococcus aureus, Bacillus subtilis, Klebsiella oxytoca, Staphylococcus epidermidis, Pseudomonas aeruginosa* and *Penicillium* sp, *Fusarium* sp, *Aspergillus niger, Candida albicans* and *Aspergillus flavus.*

2.4 Minimum Inhibitory Concentration (MIC) of methanolic extract of *P. angulata*

The Minimum inhibitory concentration (MIC) of the plant extracts on the test isolates were determined by the agar micro dilution method as described by the CLSI guidelines (M07-A6, 2003) for bacteria. The stock solutions were further diluted in a 2-fold serial dilution to obtain the following concentrations: 600, 300 and 150µg/ml. Agar plates were prepared by pouring MHA for bacterial isolates into sterile Petri plates containing 1ml of the various dilutions of the extract. The test isolates which were grown overnight in nutrient broth were adjusted to McFarland 0.5 standard and streaked onto the surface of the agar plates containing dilutions of the plant extract. The Mueller Hinton Agar plates were then incubated at 37°C for 24 hours after which all plates were observed for growth. The minimum dilution (concentration) of the extracts completely inhibiting the growth of each organism was taken as the MIC.

2.5 Qualitative and Quantitative Phytochemical Screening of *M. charantia* leaves extract

The Qualitative and Quantitative Phytochemical analysis of the leaves of methanolic extract of *P. angulata* were analyzed using the methods described by Edeoga *et al.* (2005) and were screened for the presence of the following phytochemicals: Alkaloids, Saponin, Terpenoid, Flavonoid, Cardiac glycoside and Phenol using methanol as solvent.

3.0 RESULTS

Table 1 shows the result of the antibacterial assay of *P. angulata* at various concentrations of 600, 300 and 150 ug/mL. *P. angulata* showed activity ranging from 15.50 - 05.40mm

Table 1: Antibacterial Activity of methanolic extract of *P.angulata*

Concentration (ug/mL)	**Bacterial strain**	**Plant zones of inhibition (mm)**	**Streptomycin**
600mg/ml	*Escherichia coli*	08.40	06.40
	Pseudomonas aeruginosa	11.50	08.10
	Staphylococcus aureus	10.80	09.40
	Bacillus subtilis	15.50	08.00
	Klebsiella oxytoca	05.40	04.00
	Staphylococcus epidermidis	10.40	08.40
300mg/ml	*Escherichia coli*	06.20	05.50
	Pseudomonas aeruginosa	09.20	07.00
	Staphylococcus aureus	08.70	07.50
	Bacillus subtilis	12.40	09.40
	Klebsiella oxytoca	04.80	03.20
	Staphylococcus epidermidis	08.50	07.50
150mg/ml	*Escherichia coli*	04.00	01.00
	Pseudomonas aeruginosa	06.00	04.00
	Staphylococcus aureus	07.20	06.20
	Bacillus subtilis	10.20	07.40
	Klebsiella oxytoca	03.40	02.50
	Staphylococcus epidermidis	06.50	05.50

Table 2 shows the result of the antifungal assay of *P. angulata* at various concentrations of 600, 300 and 150 ug/mL. *P. angulata* methanolic leaves extract showed antifungal activity ranging from 06.00-02.00mm.

Table 2: Antifungal Activity of methanolic extract of *P.angulata*

Concentration (ug/mL)	**Fungal strains**	**Plant zones of inhibition (mm)**	**Funamycin**
600mg/ml	*Penicillium* sp.	00.00	00.00
	Fusarium sp.	02.00	01.00
	Apergillus niger	06.00	04.00
	Candida albicans	00.00	00.00
	Aspergillus flavus	04.00	01.00
300mg/ml	*Penicillium* sp	00.00	00.00
	Fusarium sp	00.00	00.00
	Apergillus niger	04.20	03.00
	Candida albicans	00.00	00.00
	Aspergillus flavus	03.00	02.00
150mg/ml	*Penicillium* sp	00.00	00.00
	Fusarium sp	00.00	00.00
	Apergillus niger	03.20	02.40
	Candida albicans	00.00	00.00
	Aspergillus flavus	02.00	01.00

Table 3 shows the result of *P. angulata* methanolic leaves extract MIC against the bacterial isolates which ranged from 62.5-07.08 ug/mL. *Bacillus subtilis* had the highest MIC while *Klebsiella oxytoca* had the lowest concentration.

Table 3: Minimum Inhibitory Concentration (MIC) of methanolic extract of *P. angulata* against some selected bacteria

Bacterial strains	**MIC (ug/mL) Results**
Escherichia coli	15.70
Pseudomonas aeruginosa	31.30
Staphylococcus aureus	31.00
Bacillus subtilis	62.50
Klebsiella oxytoca	07.80
Staphylococcus epidermidis	31.30

Table 4 shows the result of the phytochemical (qualitative) analysis of crude methanolic extract of *P. angulata* which revealed the presence of Alkaloids, Saponin, Terpenoids, Flavonoid, Cardiac glycoside and phenol. Cardiac glycoside was the highest while alkaloid had the least value.

Table 4: Qualitative and quantitative Phytochemical analysis of ethanol extract of *P. angulata*

Bioactive compounds	**Qualitative result**	**Quantitative Results (ug /mL)**
Alkaloid	Positive	08.70±0.2
Saponin	Positive	10.35±0.2
Terpenoid	Positive	09.50±0.1
Flavonoid	Positive	10.40±0.2
Cardiac glycoside	Positive	14.40±0.1
Phenol	Positive	07.50±0.1

4.0 DISCUSSION

The antimicrobial activity results of methanolic extracts of *P. angulata* show that *P. angulata* may be susceptible to *B.subtilis, P. aeruginosa, S. aureus, S. epidermidis* and *E.coli. B. subtilis* had the highest activity while *K. oxytoca* had the lowest sensitivity at the various concentrations. The antifungal susceptibility testing was effective against *A. niger* while *Fusarium* sp had the lowest activity. *Penicillium* sp, *C. albicans and Fusarium* sp had no activity at the various concentrations. This result also agrees with the findings of Donkor *et al*. (2012) in a study of the **antimicrobial activity** of crude methanolic leaf extracts of *P. angulate that* showed activity on *S. aureus* at varying degrees. This result is in agreement with the findings of Helvaci *et al.* (2010) on antimicrobial activity of *P. alkekengi* and evaluation of antioxidant potential of *P. alkekengi* methanolic leaves extract which showed antibacterial activity against *S, aureus, S. epidermidis, E. faecalis, B. subtilis, B. cereus, E.coli, P. aeruginosa, E. cloacae, K. pneumonia*e and *P. vulgaris.* The antifungal activities showed inhibition against *C. albicans, C. krusei, C. globrata, C. tropicalis* and *C. paraphilosis.* Ushie *et al.* (2019) in a study on the antimicrobial activities of chloroform and ethyl acetate extract of *P. angulata* showed activities against *Salmonella* sp, *S. aureus,* and *E. coli*. The antifungal result show activities against *C. albicans* and *A. niger.* A study conducted by Ushie *et al.* (2019) on phytochemical and antimicrobial activities of chloroform and ethyl acetate extract of *P. angulata* show the presence of anthraquinone, glycosides, saponin, steroids, alkaloids and flavonoids. Detection of some phytochemicals in methanolic extracts of *P. angulata* is an indication that it can be used as potential source for drug formulation to treat some diseases caused by these pathogenic bacteria and fungi. The phenols have been reported to possess considerable antimicrobial properties attributed to their redox properties (Eleazu *et al.,* 2012). Flavonoids have also been reported to possess antimicrobial and anti-inflammatory properties. Alkaloids and flavonoids are responsible for the antifungal activities in higher plants (Sofowora, 2013).

4.1 CONCLUSION

Physalis angulata contain an array of bioactive compounds that can be used to treat some bacterial and fungal infections caused by these pathogenic bacteria and fungi

ACKNOWLEDGEMENT

We acknowledge Professor N.A. Amusa, of Western Union University, Okun-Owa Ogun State. Staff of Microbiology laboratory, Yaba College of Technology, staff of Pharmaceutical Research laboratory, College of Medicine, Universitv of Lagos for their contributions towards the success of this research.

REFERENCES

Clinical and Laboratory Standard Institute (CLSI) (2003). Methods for Dilution Antimicrobial Susceptibility Tests for Bacteria that Grow Aerobically. Wayne, PA: CLSI;

Damu, A.G., Kuo, P.C., Su, C.R., Kuo, T.H., Chen, T.H., Bustow, K.F., Lee, K.H. and Wu, T.S. (2007). Isolation, Structures and Structure-Cytotoxic Activity Relationships of Withanolides and Physalins from *Physalis angulata*. *Journal of Natural Products*. 70: 1146-1152.

Donkor, A.M., Glover, R.I.K., Boateng, J.K. and Akpo, V.V. (2012). Antibacterial Activity of the Fruit Extract of *P. angulata* and its Formulations. *Journal of Medical and Biomedical Sciences* 1(4): 21-26.

Edeoga, H.O., Okwu, D.E. and Mbaebie, B.O. (2021). Phytochemical Constituents of Some Nigerian Medicinal Plants. *African Journal of Biotechnology*. 4(7): 685-688.

Eleazu, C.O., Eleazu, K.C. Awa, E. and Chukwuma, S.C. (2012). Comparative Study of The Phytochemical Composition of The Leaves of Five Nigerian Medicinal Plants. *Journal of Biotechnology and Pharmaceutical Research* 3(2): 42-46.

Helvaci, S., Kokdil, M., Kowai, N., Duran, G. and Guvenc, A. (2010). Antimicrobial Activity of the Extract of Physalin D from *Physalin alkengi* and Evaluation of Antioxidant Potential of Physalin D. *Pharmaceutical Biology* 48(2): 142-150.

Kumar, R.S., Moorthy, K and Punitha, R.V. (2016). Antimicrobial Efficacy and Phytochemical Analysis of *Indigofera trita* Linn. *Journal of Traditional, Complementary and Alternative medicines.* 20:1013.

Mada, S.B., Garba, H.A., Mohammed, A., Olagunju, A. and Muhammad, A.B. (2013). Antimicrobial Activity and Phytochemical Screening of Aqueous and Ethanol Extracts of *Momordica charantia* L. Leaves. *Journal of Medicinal Plants Research*. 7(10): 579-586.

Osho, A.A., Fayemi, S.O. and Moronkola, D.O. (2010). Antimicrobial Activity of Essential Oils of *Physalis angulata* L. *African Journal of Traditional Complementary Alternative Medicine.* 7(4): 303-306.

Sandhya, V.D., Ali, S.Z., Reddy, V.G. and Grover, M. (2010). Effect of Osmotic Stress on Plant Growth Promoting *Pseudomonas* sp. *Archive of Microbiology*. 192: 867-876.

Silva, M.T.G, Simas, S.M., Batista, T.G.F.M., Cardarelli, P. and Tomassini,T.C.B. (2005) Studies on Antimicrobial Activity In-vitro of *Physalis angulata* L. (Solanacea) Fraction And PhysalinnB bringing out The Importance of Assay Determination. *Mem Inst Oswaldo Cruz100:* 100: 779-782).

Sofowora, A., Ogunbodede, E. and Onayade, O. (2013). *African Journal of Traditional Complementary and Alternative Medicines* 10(5): 210-229 2: 213-221

Soladoye, M., E. C., Olatunji, M. and Feyisola, R. (2014). Ethnobotanical Survey of Plants Used in the Treatment of Female Infertility in Southwestern Nigeria. *A Journal of Plants, People, and Applied Research, 21,* 81 - 90.

Ushie, O.A., Neji, P.A., Abeng, F.E., Okpashi, V.E., Baba, N.H. and Azuaga, T.I. (2019).

Phytochemical Screening and Antibacterial Activities of Cloroform and Ethyl Acetate

Extract of *P. angulata. Journal of Chemical Society of Nigeria* 44(6): 376.

INTERNATIONAL, JOURNAL OF SCIENCE & SOCIETY YABATECH
VOL 7, No 1, JUNE 2021. ISSN: 2276-7924

POTENTIAL OF *COULA EDULIS* SHELL CRUDE EXTRACT AS CORROSION INHIBITOR FOR MILD STEEL IN 1M H_2SO_4 SOLUTION: OPTIMIZATION USING ORTHOGONAL TAGUCHI ARRAY

Popoola, L.T.[1*], **Aderibigbe,** T. A.[2] **and Omotara,** O.O.[1]

[1]Department of Chemical and Petroleum Engineering, Afe Babalola University, Ado-Ekiti, Ekiti State.
[2]Department of Science Laboratory Technology, Yaba College of Technology, Yaba, Lagos, Nigeria.

Corresponding Author: *popoolalekantaofeek@yahoo.com*

ABSTRACT

Unique mechanical properties of mild steel make it suitable in fabrication of industrial equipment. However, mild steel quality reduces under corrosive environment which requires serious attention. In this study, crude extract of the shells of *Coula edulis* prepared using soxhlet extraction was applied as corrosion inhibitor for mild steel in 1M H_2SO_4 solution. The effectiveness of the corrosion inhibitor was investigated at different experimental conditions of temperature, inhibitor volume, pH and reaction time using the weight loss methodology. Orthogonal Taguchi array of design expert was applied as experimental design and optimization tool. Maximum corrosion inhibition efficiency of 79.66% was recorded at temperature of 60^{o}C, inhibitor volume of 20 mL, pH of 4 and reaction time of 6 hours while minimum corrosion inhibition efficiency of 40.93% was recorded at temperature of 80^{o}C, inhibitor volume of 15 mL, pH of 2 and reaction time of 6 hours. ANOVA analysis revealed a strong correlation between the experimental and predicted values of inhibition efficiency with R^2 value of 0.9915. This suggests that the developed model equation can be used as predictive tool for future inhibition efficiency prediction. The percent contribution of significant variables on the inhibition efficiency of *Coula edulis* shell extract on mild steel in 1M H_2SO_4 solution was observed to be reaction temperature (25.29%), inhibitor volume (71.37%) and reaction time (3.34%) respectively. Orthogonal design array predicted the optimum inhibition efficiency variables to be temperature of 60^{o}C, inhibitor volume of 20 mL, pH of 4 and reaction time of 2 hours respectively. Conclusively, *Coula edulis* shell extract can be effectively used as local corrosion inhibitor for mild steel in 1M H_2SO_4 solution.

KEYWORDS: Effluent, walnut shell, rice husk, adsorption, optimization

1.0 INTRODUCTION

Corrosion is the gradual destruction of materials (usually metals, ceramics or polymers) by chemical and/or electrochemical reaction with their environment (Miller, 1990). It is a phenomenon which degrades the essential properties of materials and structures including appearance, strength and permeability to liquids and gases (Popoola *et al*., 2013). Mild steel is one of the materials that has great industrial applications because of some special features it possesses such as adaptable heat treatment, weldability, strength and ductility (Akalezi *et al.* 2015). However, it is usually attacked by corrosion when subjected into different environments. Thus, it is imperative to look for better ways to control this dangerous attack.

The use of corrosion inhibitors generated from agricultural wastes in controlling corrosion of materials is becoming more trending over previously used methods that posed to be expensive and environmentally unfriendly (Popoola, 2019). Some previous studies have gotten positive results in using extracts from plants such as *Emblica officinalis* (Sanghvi *et al*., 1997), *Olea europaea* (El-Etre, 2007), *Musa sapientum* (Eddy *et al*., 2008), *Justicia gendarussa* (Satapathy *et al*., 2009), *Anthocleista djalonesis* (Ogukwe *et al*., 2012), *Dodonaea viscose* (Leelavathi *et al*., 2013), *Jatropha*

curcas (Olusegun, 2013), *Rothmannia longiflora* (Akalezi *et al*., 2015), mixed cocoa pod-Ficus exasperate (Popoola 2021) and so on as green corrosion inhibitors for mild steel in acidic media. Thus, the application of tools that will enhance the optimization of the process for better industrial application of the locally generated corrosion inhibitor is essential.

In this study, crude extract prepared using soxhlet extraction with the aid of 95% ethanol from shells of *Coula edulis* (walnut) was applied as corrosion inhibitor for mild steel in 1M H_2SO_4 solution. The effectiveness of the corrosion inhibitor was investigated at different experimental conditions of temperature, inhibitor volume, pH and reaction time using the weight loss methodology.

2.0 MATERIALS AND METHODS

2.1 Materials

Mild steel was gotten from the central engineering workshop of Afe Babalola University and the chemical composition was Fe = 98.81%, C = 0.27%, Mn = 0.68%, P = 0.061%, Si = 0.083% and Cr = 0.095%. Acetone, Ethanol, hydrochloric acid and silicon carbide paper grades were of analytical grades and purchased from Debos Scientific, Ibadan. The walnut shell was obtained as remnant from a local market in Ado-Ekiti.

2.2 Mild Steel Coupon Preparation

Silicon carbide paper was used to polish the mild steel. It was then cut into coupons of equal dimension (5×4×0.2 cm) and exposed surface area of 20 cm^2 using a digital vernier calliper. Coupons were degreased and rinsed using acetone. They were dried and kept in desiccator for weight loss experiment.

2.3 Extract Preparation

The *Coula* edulis shell was washed with water and then dried in an oven at 100^oC for 24 hours. A mechanical grinder was used to ground it into powdery form and then sieved to obtain particle size of less than 63 µm. The particles were kept in clean polythene bag and sealed to avoid moisture contamination. The sample was extracted in Soxhlet apparatus using 95% ethanol. The extract was subjected to evaporation in order to remove excess ethanol.

2.4 Batch Corrosion Experimental Design and optimization

Taguchi experimental design was applied to optimize the inhibition efficiency of *Coula edulis* shell extract on mild steel in 1M H_2SO_4 solution. The extract was added in solution to the metal in the acidic medium in a beaker to determine the corrosion rate in the presence of corrosion inhibitor. The temperature was adjusted using a temperature controlled heater. Four factors namely, temperature (60, 70 and 80^oC), inhibitor volume (10, 15 and 20 mL), pH (2, 4 and 6) and time (2, 4 and 6 hrs) were studied in this experiment. An L_9 orthogonal approach with a set of 9 experiments was applied at three levels designated as 1, 2 and 3 as shown in Table 1. The response was expressed as the percent inhibition efficiency of the crude extract. The result obtained from Taguchi design expert for the batch corrosion and optimization is presented as part of Table 2. Blank experiment was conducted without the corrosion inhibitor.

Table 1: Description of examined process variables at different levels

Variable	Description	Unit	Type	Level		
				1	2	3
T	temperature	^oC	Factor	60	70	80
I	inhibitor volume	mL	Factor	10	15	20
P	pH	-	Factor	2	4	6
t	time	hr	Factor	2	4	6
IE	Inhibition Efficiency	%	Response	-	-	-

2.5 Weight Loss Measurement

Weight loss measurement technique was used to study the optimization of the inhibition of corrosion of mild steel in 1M H_2SO_4 solution using crude extract from *Coula edulis* shell. The mild steel coupon's weight was measured before and after immersion in the medium with and without the extract used as corrosion inhibitor. The extract was added in solution to the metal in the acidic medium in a beaker. Each batch experiment was conducted based on the experimental design values. After each immersion time, mild steel coupons were removed from test solution and washed using acetone. Hot air was then used to dry the specimens and then left for some minutes to cool down. Equations 1 and 2 (Ostovari *et al*. 2009) were used to calculate corrosion rate and inhibition efficiency respectively using weight loss recorded after each experiment with the aid of digital weighing balance.

$$CR\ (mm/y) = \frac{87,500W}{A\rho t} \quad (1)$$

$$I.E.\% = \left(1 - \frac{CR_{inh}}{CR_{blank}}\right) \times 100 \quad (2)$$

Where

CR = corrosion rate (mm/y),
W = weight loss (g),
A = mild steel coupon area (cm^2),
ρ = density (g/cm^3), t = immersion time (hr),
I.E.% = inhibition efficiency,
CR_{inh} = corrosion rate in the presence of inhibitor and
CR_{blank} = corrosion rate in the absence of inhibitor.

3.0 RESULTS AND DISCUSSION

3.1 Experimental Results obtained from Batch Corrosion

The results obtained for the batch corrosion experiments conducted to check the effectiveness of the crude extract obtained from *Coula edulis* shell as corrosion inhibitor for mild steel in 1M H_2SO_4 solution is presented in Table 2. The results were obtained for the inhibition efficiency at different experimental conditions as suggested by the Taguchi experimental design. Result obtained from the weight loss approach revealed that extract from *Coula edulis* shell has potential to inhibit corrosion of mild steel in 1M H_2SO_4 solution. This shows that the *Coula edulis* shell crude extract have strong affinity to create protective barrier on mild steel surface which protects it from being
corroded in the acidic medium at different experimental conditions of temperature, inhibitor volume, pH and reaction time. Maximum corrosion inhibition efficiency of 79.66% was recorded at the second experimental run where the conditions included: temperature = 60°C, inhibitor volume = 20 mL, pH = 4 and reaction time = 6 hours while minimum corrosion inhibition efficiency of 40.93% was recorded at experimental run 8 where the conditions included: temperature = 80°C, inhibitor volume = 15 mL, pH = 2 and reaction time = 6 hours. This is a strong indication that lower reaction temperature, weak acidic solution and high inhibitor volume are favourable conditions for corrosion inhibition of mild steel in 1M H_2SO_4 solution using crude extract from *Coula edulis* shell.

Table 2. Batch experimental result to check inhibition efficiency of extract from *Coula edulis* shell on mild steel in 1M H_2SO_4 solution

Run	Temperature (ºC) *T*	Inh. Vol (ml) *I*	pH *P*	Time (hours) *t*	Inhibitor Efficiency (%)
1	70	20	2	2	67.36
2	60	20	4	6	79.66
3	80	10	6	4	44.80
4	80	20	6	2	54.66
5	70	15	6	2	63.36
6	70	10	4	6	58.76
7	60	15	4	4	72.95
8	80	15	2	6	40.93
9	60	10	2	2	71.71

3.2 Development of Mathematical Models

Four factors at three levels (low, medium and high) with orthogonal arrays generated by design-expert (7.0.0) were applied in this current study. The experimental values obtained for the inhibition efficiency of extract from *Coula edulis* shell on mild steel in 1M H_2SO_4 solution are presented in Table 3. The regression model equations (developed using Taguchi approach) stated as Equation 3 was used to establish empirical relationship between the inhibition efficiency and independent process variables. The equation is expressed as Equation 3 and was used to obtain the predicted values of inhibition efficiency as generated by the Taguchi design arrays.

Table 3. Taguchi experimental design arrays, experimental and predicted values of inhibitor efficiency

RUN	Temperature (T) (ºC)	Inhibitor Vol. (I) (ml)	pH (P)	Time (t) (hours)	Inhibitor Efficiency (%) Experimental	Predicted
1	70 [2]	20 [3]	2 [1]	2 [1]	67.36	68.94
2	60 [1]	20 [3]	4 [2]	6 [3]	79.66	78.63
3	80 [3]	10 [1]	6 [3]	4 [2]	44.80	43.77
4	80 [3]	20 [3]	6 [3]	2 [1]	54.66	54.11
5	70 [2]	15 [2]	6 [3]	2 [1]	63.36	62.33
6	70 [2]	10 [1]	4 [2]	6 [3]	58.76	58.22
7	60 [1]	15 [2]	4 [2]	4 [2]	72.95	72.4
8	80 [3]	15 [2]	2 [1]	6 [3]	40.93	42.51
9	60 [1]	10 [1]	2 [1]	4 [2]	71.71	73.29

$$\textit{Inhibition Efficiency}\ (\%) = +61.58 - 2.50T[1] + 8.47T[2] + 1.67I[1] - 13.41I[2] + 1.58t[1] - 3.16t[2] \quad (3)$$

where T, *I, P* and *t* represent temperature, inhibitor volume, pH and reaction time respectively. The values indicated the square bracket represent levels of the corresponding model terms as shown in Table 1.

3.3 Statistical Analysis and Model Fitness

The regression model equation stated as Equation 3 was used to predict value of inhibition efficiency of extract from *Coula edulis* shell on mild steel in 1M H_2SO_4 solution. The statistical analysis and model fitness are presented in Table 4. Coefficient of determination (R^2), adjusted R^2 (Adj. R^2), predicted R^2 (pred-R^2) and adequate precision are the statistical tools to check for the model fitness. The correlation between the experimental values and the predicted values which are responses from developed models were evaluated by R^2. The experimental and predicted values of corrosion inhibition efficiency were compared.

The R^2 value obtained was 0.9915 suggesting reasonable agreement between the experimental and predicted values. Value obtained indicated that 99.15% of inhibition efficiency could be described by the independent variables while only 0.85% of inhibition efficiency could not be explained by the developed model equation. Another effective tool for testing model fitness is the Adj. R^2. It uses the degree of freedom measurement on its calculations to correct R^2-value for the sample size in the model. Adj-R^2 values, apparently smaller than R^2, suggest presence of irrelevant terms in the developed models with very small sample size. In this current study, the Adj-R^2 values obtained was 0.9661 which is very close to the R^2-value. Nevertheless, the pred-R^2 of 0.8284 shows reasonable agreement with Adj-R^2 value. The signal to noise ratio is a function of the Adeq precision with a ratio greater than 4 to be desirable. There were strong indications of adequate signal as value of adeq precision obtained was 17.071.

The results of the analysis of variance (ANOVA) for the fit of inhibition efficiency from Taguchi design are presented in Table 4.3. The significance of developed model and its accuracy is usually examined with the aid of ANOVA. In this study, the F-values of developed models is obtained as 39.01 signifying the accuracy of the model.

Furthermore, the significance of model variables are measured by respective values of Prob > F (*p*-value). A value less than 0.05 means variables are significant. In this current work, the significant model terms for inhibition efficiency of *Coula edulis* shell extract on mild steel in 1M H_2SO_4 solution are temperature, inhibitor volume and reaction time with *p*-value of 0.0327, 0.0118 and 0.2039 respectively.

Table 4. Analysis of variance (ANOVA) for modified effect for inhibition efficiency

Source	sum of Squares	df	Mean Square	F-Value	p-value Prob > F	% Contribution
Model	1347.63	6	224.61	39.01	0.0252	Significant
T	340.82	2	170.41	29.60	0.0327	25.29
I	961.86	2	480.93	83.53	0.0118	71.37
t	44.96	2	22.48	3.90	0.2039	3.34
Residual	11.52	2	5.76			
Cor Total	1359.15	8				
R-Squared	0.9915					
Adj R-Squared	0.9661					
Pred R-Squared	0.8284					
Adeq Precision	17.071					

3.4 Percent Contribution of Significant Process Variables

Equation 4 was used to calculate the percent contribution of each of the significant process variables. The calculated values are included in Table 4. Among the selected variables, reaction temperature (25.29%), inhibitor volume (71.37%) and reaction time (3.34%) significantly affect inhibition efficiency of *Coula edulis* shell extract on mild steel in 1M H_2SO_4 solution.

$$Percentage\ contribution = \left[\frac{SS_i}{\sum SS_i}\right] \times 100\% \left(i \neq 0\right) \qquad (4)$$

where SS_i = Sum of square of significant parameter.

3.5 Optimization of Inhibition Efficiency of *Coula edulis* shell extract on mild steel in 1M H_2SO_4 solution

The optimization of process variables was executed in order to determine the favorable process conditions required for maximum inhibition efficiency of *Coula edulis* shell extract on mild steel in 1M H_2SO_4 solution. Among the four independent variables examined for this study, solution pH was found to be insignificant for optimum inhibition efficiency and thus, its value was placed at minimum value of 2 while other variables are optimized. Table 5 presents the predicted and validated values of inhibition efficiency at optimum values. The experiment was conducted in triplicate to ensure certainty of the validated predicted optimum value. The result revealed that the model developed is efficient to predict the process responses excellently as experimental and predicted values are closer to each other.

Table 5. Optimum Point Prediction and Validation

Inhibition Efficiency	Optimum Points				% Optimum Removal	
	P	T (^{o}C)	I (mL)	t (hr)	Predicted	Experimental
%	2 [1]	60 [1]	20 [3]	2 [1]	74.16	72.56 ± 0.03

4.0 CONCLUSION

In this study, crude extract prepared using soxhlet extraction from shells of *Coula edulis* with the aid of 95% ethanol was applied as corrosion inhibitor for mild steel in 1M H_2SO_4 solution. The effectiveness of the corrosion inhibitor was investigated at different experimental conditions of temperature, inhibitor volume, pH and reaction time using the weight loss methodology. Orthogonal Taguchi array of design expert was applied as experimental design and optimization tool. Maximum corrosion inhibition efficiency of 79.66% was recorded at temperature of 60^{o}C, inhibitor volume of 20 mL, pH of 4 and reaction time of 6 hours while minimum corrosion inhibition efficiency of 40.93% was recorded at temperature of 80^{o}C, inhibitor volume of 15 mL, pH of 2 and reaction time of 6 hours. ANOVA analysis revealed a strong correlation between the experimental and predicted values of inhibition efficiency with R^2 value of 0.9915. This suggests that the developed model equation can be used as predictive tool for future inhibition efficiency prediction. The percent contribution of significant variables on the inhibition efficiency of *Coula edulis* shell extract on mild steel in 1M H_2SO_4 solution was

observed to be reaction temperature (25.29%), inhibitor volume (71.37%) and reaction time (3.34%) respectively. Orthogonal design array predicted the optimum inhibition efficiency variables to be temperature of 60^{o}C, inhibitor volume of 20 mL, pH of 4 and reaction time of 2 hours respectively. Conclusively, *Coula edulis* shell extract can be effectively used as local corrosion inhibitor for mild steel in 1M H_2SO_4 solution.

REFERENCES

Akalezi CO, Oguzie EE, Ogukwe CE, Ejele EA (2015) Rothmannia longiflora extract as corrosion inhibitor for mild steel in acidic media. *International Journal of Industrial Chemistry*, 6(4):273–284.

Eddy NO, Ebenso EE (2008) Adsorption and inhibitive properties of ethanol extracts of *Musa sapientum* peels as a green corrosion inhibitor for mild steel in H_2SO_4. *Afr J Pure Appl Chem*, 2(6):046–054.

El-Etre AY (2007) Inhibition of acid corrosion of carbon steel using aqueous extract of olive leaves. *Journal of Colloid and Interface Science*, 314:578-583.

Leelavathi S, Rajalakshmi R (2013) *Dodonaea viscosa* leaves extract as acid corrosion inhibitor for mild Steel – A Green approach. *JMES*, 4(5):625–638.

Miller D (1990) Corrosion control on aging aircraft: what is being done?, Mater Perform, 29, 1990, 10–11.

Ogukwe CE (2012) Corrosion inhibition and adsorption of *Anthocleista djalonesis* leaf extract on the acid corrosion of mild steel. *Portugaliae Electrochimica Acta*, 30(5):189–202.

Olusegun SJ (2013) Jatropha curcas leaves extract as corrosion inhibitor for mild steel in 1M hydrochloric acid. *Journal of Emerging Trends in Engineering and Applied Sciences*, 4(1):138–143.

Ostovari A, Hoseinieh SM, Peikari M, Shadizadeh SR, Hashemi SJ (2009) Corrosion inhibition of mild steel in 1 M HCl solution by henna extract: A comparative study of the inhibition by henna and its constituents (lawsone, gallic acid, α-D-glucose and tannic acid). *Corros Sci*, 51:1935–1949.

Popoola LT (2019) Progress on pharmaceutical drugs, plant extracts and ionic liquids as corrosion inhibitors. *Heliyon*, 5, e01143.

Popoola LT, Grema AS, Latinwo G, Gutti B, Balogun A (2013) Corrosion problems during oil and gas production and its mitigation. *Int. J. Ind. Chem.*, 4(1):35-50.

Popoola, LT (2021) Corrosion inhibitory effect of mixed cocoa pod-Ficus exasperata extract on MS in 1.5 M HCl: Optimization and Electrochemical Study. Corros Rev 2021; aop doi.org/10.1515/corrrev-2019-0077

Sanghvi MJ, Shuklan SK, Misra AN, Padh MR, Mehta GN (1997) Inhibition of hydrochloric acid corrosion of mild steel by aid extracts of Embilica officianalis, Terminalia bellirica and Terminalia chebula. *Bull Electrochem*, 13(8–9):358–361.

Satapathy AK, Gunasekaran G, Sahoo SC, Amit K, Rodrigues PV (2009) Corrosion inhibition by Justicia gendarussa plant extract in hydrochloric acid solution. *Corros. Sci.*, 51:2848-2856.

A COMPARATIVE ANALYSIS ON THE PERFORMANCE OF RIDGE, LASSO AND ELASTIC NET REGRESSION MODEL IN TERMS OF FLEXIBILITY

*Nwajieze C. O.[1], Onyenekwe C. E.[2], Olufolabo A.A.[3], and Olufolabo O.O.[1]

[1]Department of Statistics, Yaba College of Technology, Yaba Lagos State
[2]Department of Statistics, Nnamdi Azikiwe University, Awka, Anambra State
[3]Federal School of Statistics, Ibadan, Oyo State

Corresponding Author E-mail: nwajieze@gmail.com

ABSTRACT

Prediction remains one of the fundamental reasons for regression analysis. In satisfying the assumptions of regression analysis such as collinearity between explanatory variables is a significant issue in data science. Classical Linear Regression Model (CLRM) do show higher correlation coefficients, its estimate not stable and the predictive model developed may be inaccurate due to collinearity problem that always leads to over fitting. Advanced level methods or penalized regression such as Ridge, Lasso and Elastic net regression methods are designed to overcome such problem. This work is therefore gear towards finding the best penalized regression model for predicting and modeling of Nigeria's economic data. Using the Nigerian economic data from NBS and using Root Mean Square Error (RMSE) to compare the three methods, Ridge regression has RMSE value of 0.0307, Lasso has 0.0290 and Elastic net has 0.0302. This implies that Lasso regression performs better than both Ridge and Elastic net regression on Nigerian economic data. The analysis was done using the R software for statistical computing.

KEYWORDS:

Root Mean Square Error, Ridge, Lasso, Elastic Net, Validation of estimates.

INTRODUCTION

The gross domestic product (GDP) is one of the primary indicators used to gauge the health of a country's economy. It represents the total money value of all goods and services produced over a specific time period; you can think of it as the size of the economy. Usually, GDP is expressed as a comparison to the previous quarter or year. For example, if the year-to- year GDP is up 5%, this is thought to mean that the economy has grown by 5% over the last year. The expenditure method is the more common approach and is calculated by adding total consumption, investment, government spending and net exports.

Typically, a simple model such as linear regression may fail in mapping the underlying concept due to collinearity and too complex ones such as generalized regression tend to over fit the data due to lack of functional link and collinearity as well Hastie et al (2017); Guyon and Elisseeff (2003). Often the traditional regression model can show higher correlation coefficients, but can suffer from over fitting and its lower prediction accuracy Aleixandre-Tudo et al (2015). One of the ways of avoiding over fitting is using cross validation that helps in estimating the error over test data set, and in deciding what parameters work best for your model Mayooran et al (2019).

Regularization process imposes an upper threshold on the values taken by the coefficients that constrains or shrinks the coefficient estimates towards zero especially for the variables which influence the over fitting. Mayooran et al (2019) In data science, the analyst might be interested in the esti-mated values for the objects in the training set, predicting responses for new objects. However, identifying which input variables are most important in making good predictions, is challenging due to complex relations between these variables Rahman, A. (2008)

The aim of this research is to determine the best penalized regression model for

predicting and modeling of Nigeria's economic data as supervised statistical learning problems with specific objectives to:
i. Explore the strength and weaknesses of the penalized regression models.
ii. The comparing of the models for the selection of best penalized model among the three models for prediction
iii. To Perform prediction on the best selected model
iv. To determine the economic relationship between each economic indices.

The study provides better understand to the relationship that exists between GDP and other sectors of the economy and it explains the role of all indices and their contributions to the economy.

METHODOLOGY

Ridge Regression technique

Don't forget that the least squares fitting procedure estimates $\beta_0, \beta_1, \dots, \beta_p$ using the values that minimize

$$RSS = \sum_{i=1}^{n}\left(y_i - \beta_0 - \sum_{j=i}^{p}\beta_j x_{ij}\right)^2 \qquad (1)$$

Ridge regression as invented by Hoerl and Kennard (1970) is very similar to least squares, except that the coefficients are estimated by minimizing a slightly different quantity. In particular, the ridge regression coefficient estimates $\hat{\beta}^R$ are the values that minimize

$$\sum_{i=1}^{n}\left(y_i - \beta_0 - \sum_{j=i}^{p}\beta_j x_{ij}\right)^2 + \lambda\sum_{j=1}^{p}\beta_j^2 \qquad (2)$$

that is $RSS + \lambda\sum_{j=i}^{p}\beta_j^2$
where $\lambda \geq 0$ is a tuning parameter, to be determined separately. As with least squares, ridge regression seeks coefficient estimates that fit the data well, by making the **RSS** small. However, the second term, $\lambda\sum_j \beta_j^2$, called a shrinkage penalty, is small when $\beta_1, \dots, \beta_p$ are close to zero, and so it has the effect of shrinking the estimates of β_j towards zero. The tuning parameter A serves to control the relative impact of these two terms on the regression coefficient estimates. When $\lambda = 0$, the penalty term has no effect, and ridge regression will produce the least squares estimates. However, as $\lambda \to \infty$, the impact of the shrinkage penalty grows, and the ridge regression coefficient estimates will approach zero. Unlike least squares, which generates only one set of coefficient estimates, ridge regression will produce a different set of coefficient estimates, $\hat{\beta}_\lambda^R$, for each value of λ. Selecting a good value for A is critical. The shrinkage penalty is applied to $\beta_1, \dots, \beta_p$, but not to the intercept β_0. We want, to shrink the estimated association of each variable with the response; however, we do not want to shrink the intercept, which is simply a measure of the mean value of the response when $x_{i1} = x_{i2} = \cdots = x_{ip} = 0$. If we assume that the variables; that is, the columns of the data matrix X have been centered to have mean zero before ridge regression is performed, then the estimated intercept will take the form $\beta_0 = \bar{y} = \sum_{i=1}^{n}\frac{y_i}{n}$

Lasso Regression technique

Ridge regression does have one obvious disadvantage. Unlike best subset, forward stepwise, and backward stepwise selection, which will generally select models that involve just a subset of the variables, ridge regression will include all p predictors in the final model. The penalty $\lambda\sum\beta_j^2$ in (2) will shrink all of the coefficients towards zero, but it will not set any of them exactly to zero (unless $\lambda = \infty$). This may not be a problem for prediction accuracy, but it can create a challenge in model interpretation in settings

in which the number of variables p is quite large. So we might wish to build a model including just these predictors. However, ridge regression will always generate a model involving all the predictors. Increasing the value of λ will tend to reduce the magnitudes of the coefficients, but will not result in exclusion of any of the variables. The lasso as invented by Tibshirani (1996) is a relatively recent alternative to ridge regression that overcomes this disadvantage. The lasso coefficients, $\hat{\beta}_\lambda^L$, minimize the quantity

$$\sum_{i=1}^{n}\left(y_i-\beta_0-\sum_{j=i}^{p}\beta_j x_{ij}\right)^2+\lambda\sum_{j=1}^{p}\left|\beta_j\right| \qquad (3)$$

that is $RSS+\ \lambda\sum_{j=1}^{p}\left|\beta_j\right|$

Comparing (2) to (3), we see that the lasso and ridge regression have similar formulations. The only difference is that the β_j^2 term in the ridge regression penalty (2) has been replaced by $\left|\beta_j\right|$ in the lasso penalty (3).

In statistical parlance, the lasso uses an ℓ_1 (pronounced 'ell 1') penalty instead of an ℓ_2 penalty. The ℓ_1 norm of a coefficient vector β is given by $\|\beta\|_1=\sum\left|\beta_j\right|$. As with ridge regression, the lasso shrinks the coefficient estimates towards zero. However, in the case of the lasso, the ℓ_1 penalty has the effect of forcing some of the coefficient estimates to be exactly equal, to zero when the tuning parameter λ is sufficiently large. Hence, much like best subset selection, the lasso performs variable selection. As a result, models generated from the lasso are generally much easier to interpret than those produced by ridge regression. We say that the lasso yields sparse models, that is; models that involve only a subset of the variables. As in ridge regression, selecting a good value of λ for the lasso is critical.

Elastic net regression technique

Elastic net linear regression as invented by Zou and Hastie (2005) uses the penalties from both the lasso and ridge techniques to regularize regression models. The technique combines both the lasso and ridge regression methods by learning from their shortcomings to improve on the regularization of statistical models. The elastic net method improves on lasso's limitations, i.e., where lasso takes a few samples for high dimensional data, the elastic net procedure provides the inclusion of 'n' number of variables until saturation.

$$\sum_{i=1}^{n}\left(y_i-\beta_0-\sum_{j=i}^{p}\beta_j x_{ij}\right)^2+\lambda\left[(1-\alpha)\sum\beta^2+\alpha\sum|\beta|\right] \qquad (4)$$

if $\alpha=\ 0$ then. (4) is ridge regression while if $\alpha=1$ then (4) becomes Lasso regression. In a case where the variables are highly correlated groups, lasso tends to choose one variable from such groups and ignore the rest entirely. To eliminate the limitations found in lasso, the elastic net includes a quadratic expression ($\|\beta\|^2$) in the penalty, which, when used in isolation, becomes ridge regression. The quadratic expression in the penalty elevates the loss function toward being convex. The elastic net draws on the best of both worlds i.e., lasso and ridge regression. In the procedure for finding the elastic net method's estimator, there are two stages that involve both the lasso and regression techniques. It first finds the ridge regression coefficients and then conducts the second step by using a lasso sort of shrinkage of the coefficients. This method, therefore, subjects the coefficients in two types of shrinkages. The double shrinkage from the naÃŕve version of the elastic net causes low efficiency in predictability and high bias. To correct, for such effects, the coefficients are rescaled by multiplying them by $(1+\lambda_2)$.

Elastic Net Regularization

During the regularization procedure, the ℓ_1 section of the penalty forms a sparse model. On the other hand, the quadratic section of the penalty makes the ℓ_1 part more stable in the path to regularization, eliminates the quantity limit of variables to be selected, and promotes the grouping effect. The grouping effect helps the variables to be easily identified using correlation. That enhances the sampling procedure. It also increases the number of variables selected, since when one variable is sampled in a highly correlated group, all the other variables in that group are automatically added into the sample.

Variables Selection

Model building requires variables selection to form a subset of predictors. Elastic net uses the $p \gg n$ problem approach, which means that the number of predictors' numbers is higher than the number of samples used in the model. Elastic net is appropriate when the variables form groups that contain highly correlated independent variables. Variable selection is incorporated into the model-building procedure to aid in raising the accuracy. In the case where a group of variables is highly correlated and one of the variables is selected into the sample, the whole group is automatically included in the sample.

Cross-validation of Ridge and Lasso

Cross-validation is an appropriate method to find a 'most suitable' estimate for the λ parameter with a given data set. Typically, λ values that are too small can lead to over fitting when the model would tend to describe the noise in the data. On the other side, large λ values would lead to under fitting when the procedure cannot capture the underlying relationship. To perform cross validation, first the initial data set is randomly divided into K blocks of equal length. One of the blocks is assigned the role of the test set while the remaining 1 blocks together constitute the train set. In practice the number of blocks is usually selected to be 5 or 10. Next we choose a grid of values $\lambda = \lambda_s$ and calculate the regression coefficients for each λ_s value. Given these regression coefficients, we then compute the residual sum of squares.

$$RSS_{\lambda_s}k = \sum_{i=1}^{n}\left(y_i - \sum_{j=1}^{k-1}\hat{\beta}(k,\lambda_s)x_{ij}\right)^2 \qquad (5)$$

where $k = 1,\ldots.k$ is the index of the block selected as the test set. One can obtain the average of these **RSS** values over all blocks.

$$MSE_{\lambda_s} = \frac{1}{k}\sum_{k=1}^{k} RSS_{\lambda_s}k \qquad (6)$$

λ is then set equal to λ_s, that gives the minimum MSE_{λ_s}. Second popular approach utilizes the 'one-standard-error rule'. For each MSE_{λ_s} the standard error of the mean is calculated. Then the largest λ_s is selected for which MSE_{λ_s} is within one standard error of the minimum MSE value. This way we get a 'more regularized' model while increasing the MSE by not more than one standard error.

RESULTS

Data Summary

The Nigeria economic data set used for this research is gotten from the site of Nigeria Bureau of Statistics (NBS) website www.nigerianstat.gov.ng. The economic data set describes the economic activities in Nigeria and their contributions to the Gross Domestic Product (GDP). In this work, we only analyze the economic data by considering the 18 economic predictors p = 18 which encompasses the economic activities in the country for 38 years n = 38 that is, 1981-2018. We build regression models that describe how the GDP quality score depends on the economic indices characteristics of the data using Ridge, Lasso and Elastic Net. We use R software for all calculations, namely its glmnet package.

Ridge Regression plot

Ridge plot

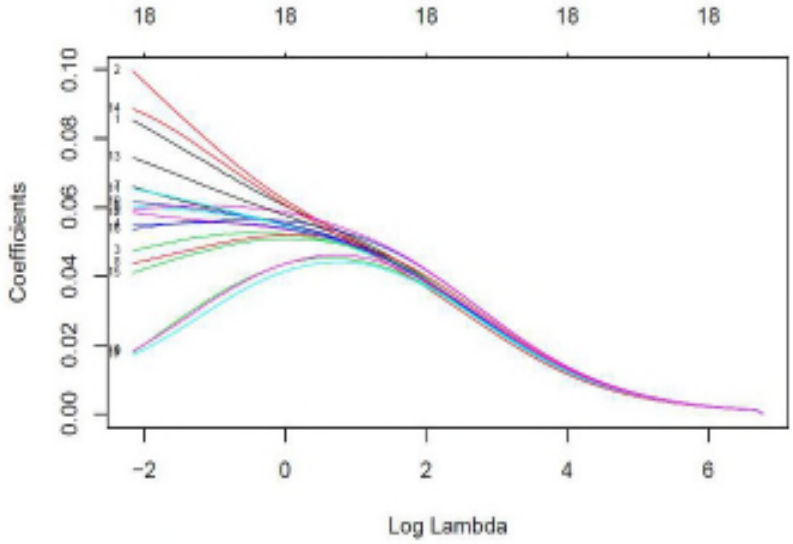

Figure 1: ridge plot

The plot (figure 1) above shows that when log lambda is at about 8, all the coefficients are more or less zero and as Lambda is (relaxed) reduced, the coefficient of variable starts to grow and as it grows, the sum of squares of the coefficients are likely to become larger. At the top of the plot, it shows that at every point we have all 18 predictive variables in the model. So increasing lambda helps to reducing the size of the coefficients, it does not make the coefficients of those that are not contributing zero.) Coefficients of other X variables increase as Lambda reduces, this means that the coefficient that does not increase rapidly as Lambda is reduced performs better in the model to the one that increases rapidly

Ridge Regression Model

Now, fitting the Ridge regression model for the data set, (train set). We want to choose λ large enough to provide stable coefficients, but not unnecessarily large ones, as this introduces additional bias and increases the residual mean square.

This study uses cross validation method for estimated λ. The figure 2 depicts the mean squared prediction error against log (λ). The gray bars at each point show MSE plus and minus one standard error (Interval). One of the vertical dashed lines shows the location of the minimum of MSE. The second dashed line shows the point selected by the one-standard-error rule. Using the cross-validation results, we now get proper values for log (λ). In this case R programming gives that exact proper λ values ridge.bestlam (i.e. Ridge$\lambda best$) = 0.1723006 and ridge.lam1se (i.e. Ridge$\lambda 1se$) = 0.3980367. It is apparent that the mean squared prediction errors are fairly large for a high value of log (λ).

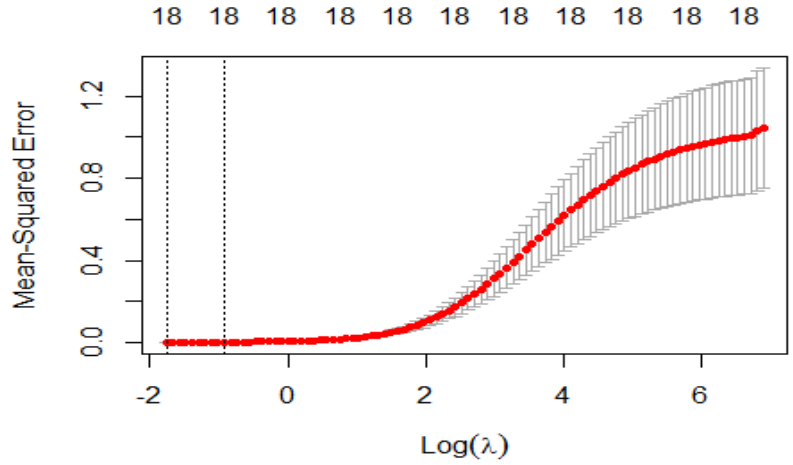

Figure 2: Cross-validated estimate of the mean square error for Ridge

Lasso regression plot

Lasso plot

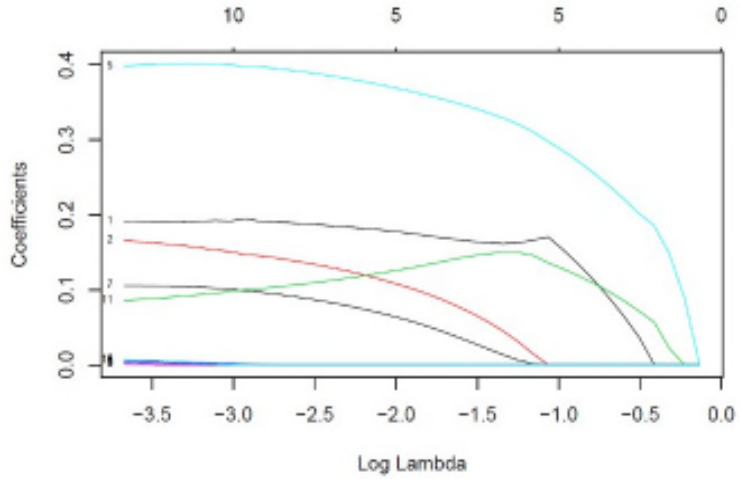

Figure 3: lasso plot

The plot above (figure 3) shows that when log lambda is at about -0.2, all the coefficients are more or less zero, and as Lambda is (relaxed) reduced, not all the coefficient of variable starts to grow because some have been shrunk to zero and some parameters grows, the sum of squares of the coefficients will become larger. At the top of the plot, it shows that at the point where lambda is relaxed to -2.0 only 5 predictive variables were in the model and as lambda is relaxed the more, more predictive variables will be in the model which will lead to overfitting. So increasing lambda helps to reduce the size of the coefficience, it makes the coeffience of those that are not contributing zero. Coefficient of other predictive variables increase as Lambda is reduced. The coefficient of variable in blue colour starts to grow rapidly while coefficient of variable in red, black etc. grows gradually as lambda is relaxed, this means that the coefficient that does not increase rapidly as Lambda is reduced performs better in the model to the one that increases rapidly.

Lasso Regression Model

Next, we fit the Lasso regression model for white wine data (train set). The figure 4 below depict the mean squared prediction error against log (λ). Using the cross-validation results, we now get proper values for Lasso model as λ values lasso. bestlam (i.e. Lasso$\lambda best$) = 0.02874147 and lasso.lam1se (i.e. Lasso$\lambda 1se$) = 0.0346192. Graph shows that the mean squared prediction errors are dramatically increasing with the log (λ) value of around -3.4.

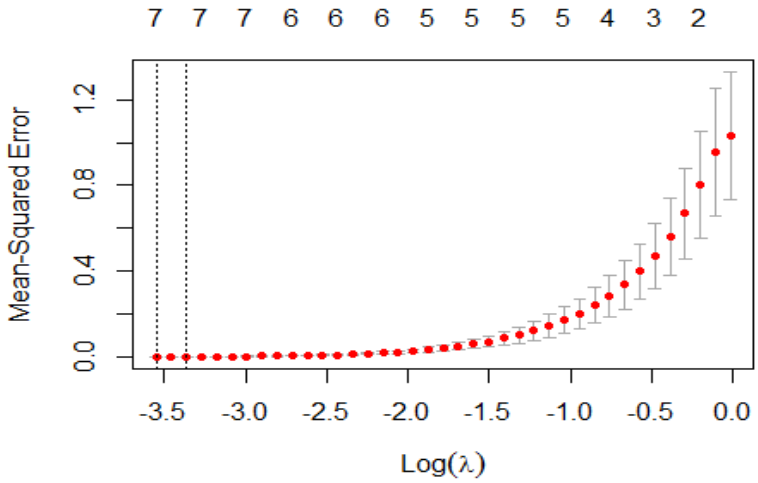

Figure 4; Cross-validated estimate of the mean square error for Lasso

Elastic Net Regressio

Elastic Net plot

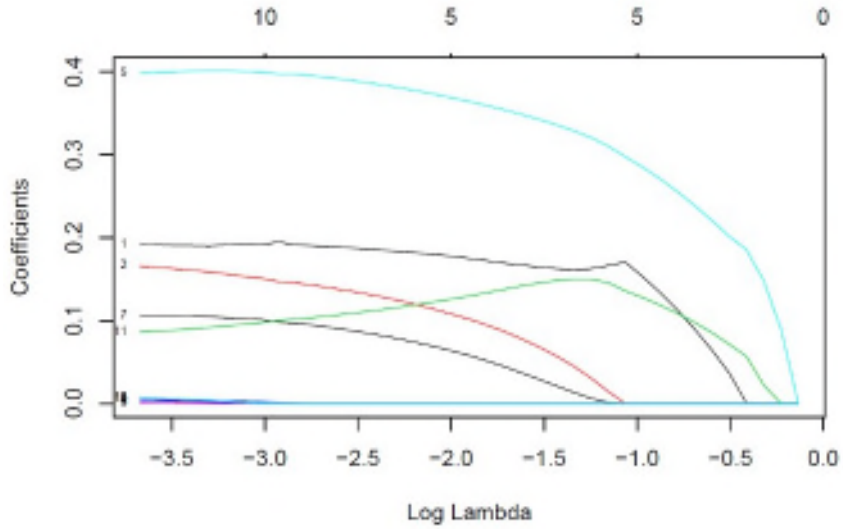

Figure 5; Elastic Net plot

The (figure 5) plot above shows that when log lambda is at about -0.2, all the coefficients are more or less zero, and as Lambda is (relaxed) reduced, not all the coefficient of variable starts to grow because some have been shrunk to zero and some parameters grows, the sum of squares of the coefficience will become larger. At the top of the plot, it shows that at the point where lambda is relaxed to -2.0 only 5 predictive variables were in the model and as lambda is relaxed the more, more predictive variables will be in the model which will lead to overfitting. So increasing lambda helps to reduce the size of

the coefficience, it makes the coeffience of those that are not contributing zero. Coefficient of other predictive variables increase as Lambda is reduced. The coefficient of variable in blue colour starts to grows rapidly while coefficient of variable in red, black etc. grows gradually as lambda is relaxed, this means that the coefficient that does not increase rapidly as Lambda is reduced performs better in the model to the one that increases rapidly.

Note that it is a coincident that the Lasso and Elastic net plot looks same

.

Elastic Net Regression Model

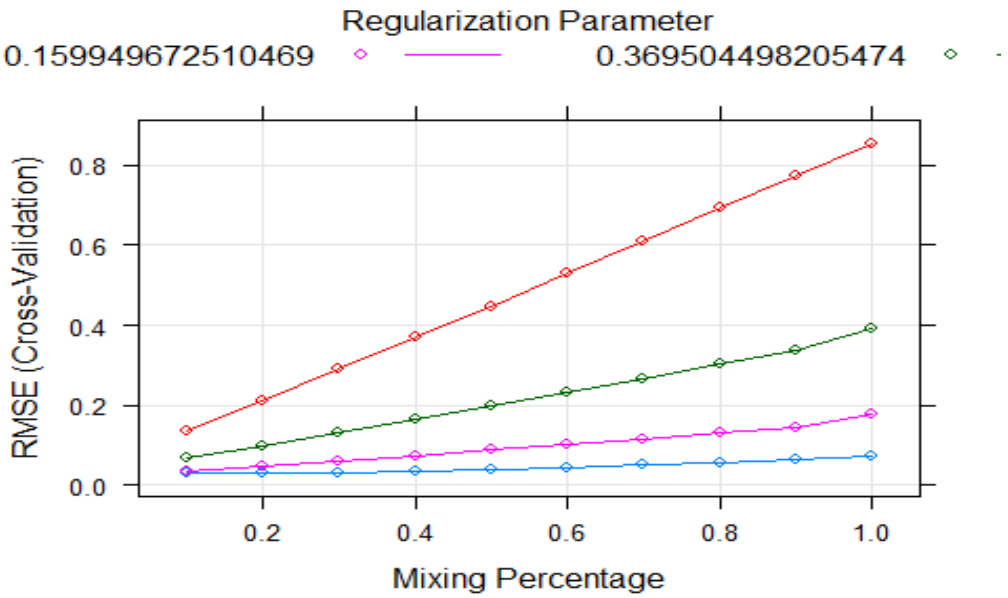

Figure 6; Elastic Net model plot

The lines in figure 6 above are lines of regularization parameter values starting from 0 to 1 and it shows that the root mean square of the line in red is higher compared to the once below i.e the lines in green, blue and purple, and it decreases in that order.

Comparing results

In this section, we are comparing all the three models by using RMSE. First we estimated λ values based on train data sets by using two cross validation. Then we apply our estimated λ values in train data for estimating coefficients from Ridge, Lasso Elastic Net models. Results are presented in table 1. The estimated coefficient values especially for the Lasso model tends to converge to zero for some parameters.

Table 1: Coefficient estimates for the economic data set for penalized regression techniques (train set)

variable	Coef	$Ridge_{\lambda best}$	$Ridge_{\lambda 1se}$	$Lasso_{\lambda best}$	$Lasso_{\lambda 1se}$	ElasticNet
Constant	$\hat{\beta}_0$	-0.0027	-0.0032	-0.0010	-0.0022	-0.0026
Agriculture	$\hat{\beta}_1$	0.0767	0.0659	0.2674	0.3138	0.0901
Industry	$\hat{\beta}_2$	0.0837	0.0694	0.1536	0.1729	0.1016
Manufacturing	$\hat{\beta}_3$	0.0520	0.0505	0.1069	0.0097	0.0529
Construction	$\hat{\beta}_4$	0.0475	0.0464	0.0000	0.0000	0.0467
Trade	$\hat{\beta}_5$	0.0574	0.0544	0.3242	0.2225	0.0609
Transport	$\hat{\beta}_6$	0.0519	0.0508	0.0000	0.0000	0.0510
Infor...Comm	$\hat{\beta}_7$	0.0597	0.0565	0.1260	0.1062	0.0667
Utilities	$\hat{\beta}_8$	0.0433	0.0462	0.0000	0.0000	0.0380
Accom...Food.Serv	$\hat{\beta}_9$	0.0384	0.0434	0.0000	0.0844	0.0293
Fin...Insur	$\hat{\beta}_{10}$	0.06620	0.0624	0.0000	0.0005	0.0699
Real.Estate	$\hat{\beta}_{11}$	0.0695	0.0660	0.0000	0.0000	0.0716
Prof..Sci...Tech.Serv.	$\hat{\beta}_{12}$	0.0518	0.0546	0.0002	0.0030	0.0503
Admin...Sup.Serv.Bus.Serv	$\hat{\beta}_{13}$	0.0671	0.0644	0.00001	0.0000	0.0711
Public.Administration	$\hat{\beta}_{14}$	0.0871	0.0785	0.0000	0.0000	0.0829
Education	$\hat{\beta}_{15}$	0.0408	0.0481	0.0000	0.0000	0.0365
Human.Health...Soc.Serv	$\hat{\beta}_{16}$	0.0564	0.0580	0.0000	0.0000	0.0538
Arts..Entert...Recr	$\hat{\beta}_{17}$	0.0196	0.0318	0.0000	0.0000	0.0000
Other.Services	$\hat{\beta}_{18}$	0.0283	0.0361	0.0000	0.0000	0.0099

As can be seen, ridge and lasso models produce a more regularized model in the sense that the coefficient estimates get more 'shrunk' towards zero when λ best values moves to λ1se . In case of
Lasso, the coefficients β4, β6, β8 β11 β13, β14, β15, β16, β17 and β18 becomes equal to zero which makes it easier for interpretation as compare to ridge regression and Elastic net.

To compare the performance of all models, we calculate the RMSE on the test set. The root mean squares error (RMSE) values for all the methods are given in table 2. From the table of coefficient estimates for the economic data
above, it is clear that the advantage of lasso over ridge is evident as it shrinks some coefficient to exact zero and makes it easier for interpretation of the model

Table 2: Comparing model prediction performance using RMSE and R-SQUARE values

Model	RMSE	R-SQUARE
Ridge	0.0815	0.9954
Lasso	0.0402	0.9999
Elastic net	0.0533	0.9986

The table 2 above shows the prediction performance of the models, about 99.54% of variations in the data where explained by the ridge regression model with RMSE 0.0815 while about 99.99% of the total variations was explained by Lasso with RMSE 0.0402 and about 99.86% of the total variations where also explained by Elastic Net with RMSE 0.0533. This therefore means that more variations where explained by Lasso model and having the lowest RMSE as compared to Ridge and Elastic Net

Table 3: Comparing Model Performance

Model	RMSE
Ridge	0.0307
Lasso	0.0290
Elastic Net	0.0302

Using the Nigerian economic data from NBS, it is very clear that Lasso model performed better than both ridge and elastic net model using Root Mean Square Error (RMSE) to compare the three methods. Ridge regression has RMSE value of 0.0307, Lasso has 0.0290 and Elastic net has 0.0302. This implies that Lasso regression performs better than both Ridge and Elastic net regression on Nigerian economic data with the lowest mean RMSE as shown in table 3 and in table A1 in appendix

CONCLUSION

The Ridge regression tends to shrink coefficients close to zero, the Lasso and Elastic Net tend to shrink to zero coefficient estimates in the sense that they reduce the norm of the estimate vector as λ increases. The Ridge regression does not produce zero estimates even for large values of λ. The lasso regression performs variable selection and it tends to shrink some of the coefficient estimates exactly to zero, which makes the regression model easier to interpret as compared to Ridge. The RMSE value calculated on the test set for Lasso is less than that for Ridge and Elastic Net when λ is selected appropriately. Calculating the RMSE on the test data set provides a good way to assess the regression model in contrast to using a single data set. We can apply our result for several variety of data sets. But note that regularized models perform better on high dimensional data set.

REFERENCES

Aleixandre-Tudo J. L., Alvarez I., Garcia M. J., Lizama V., and Aleixandre L. J. (2015) Application of multivariate regression methods to predict sensory quality of red wines. Czech J. Food Sci.,vol.61, no.33,pp.217-227.

Chowdhury M., Rahman A., and Islam R. (2018). Malware analysis and detection using data mining and machine learning classification Advances in Intelligent Systems and Computing,580 266-274

Friedman J., Hastie T., and Tibshirani R. (2010) Regularization paths for generalized linear models via coordinate descent. Journal of Statistical Software, no.33,pp.1-22

Gareth, J., Daniela, W., Hastie, T and Tibshirani, R (2013) An Introduction to Statistical Learning, with Applications in R. Springer

Guyon I., and Elisseeff A. (2003) An introduction to variable and feature selection. Journal of Machine Learning Research 3 1157-1182

Hastie T., Tibshirani R. and Friedman J. (2017) The Elements of Statistical Learning: Data Mining, Inference, and Prediction.(2nd ed) New York: Springer-Verlag.

Hastie T., Tibshirani R. and Wainwright M. (2015) Statistical learning with sparsity: The Lasso and generalizations. Chapman Hall, London

James J., Witten D., Hastie T. and Tibshirani R. (2013) An Introduction to Statistical Learning with Applications in R Springer, NY

kassambara, A. (2017) Machine Learning Essentials; Practical Guide in R (1st ed) STHDA http://www.sthda.com

Liu, H. and Zhang, J. (2009) Estimation consistency of the group Lasso and its applications. J Mach Learn Res Workshop Conf Proc. 53376-83.

Mayooran, T.. (2018) Gradient-based optimization algorithm for ridge regression by using R. International Journal of Research and Scientific Innovation 5438-44

Mayooran, T, Azizur, R and Mathew, G. (2019) Recent Developments in Data Science: Comparing Linear, Ridge and Lasso Regressions Techniques Using Wine Data DISP ’19, Oxford, United Kingdom

Meier, L., Van de Geer, S., and Buhlmann, P. 2008) The group Lasso for logistic regression. J R Stat Soc Ser B. 7053-71

Montgomery, D. and Peck, V. (2012) Introduction to linear regression analysis (5th ed) John Wiley Sons, Inc., London

Rahman, A. (2008) Bayesian predictive inference for some linear models under Student-t errors VDM-Verlag, Saarbrucken

Zhang H., Wahba G., Lin Y., Voelker M., Ferris M., Klein R., and Klein B. (2002) Variable selection and model building via likelihood basis pursuit. Technical Report 1059, University of Wisconsin, USA.

THE NUMBER OF CHAINS OF SUBGROUPS OF THE *HEISENBERG* GROUP

Ogiugo, M.E. [1], Ige, S.A [2] and Enobabor, O.E.[3]

[1, 2,3] Department of Mathematics, Yaba College of Technology, Lagos, Nigeria
Corresponding Author: mike.ogiugo@yabatech.edu.ng

ABSTRACT

In this paper, we determined an explicit formula for the number of chains of subgroups in the subgroup lattice of the Heisenberg group where p is a prime. The Heisenberg group is the unique non-abelian group of order p^3 of exponent p. It is a group of order p^3 with generators x, y and relations: $\boldsymbol{xp = yp = zp = 1, xz = zx, yz = zy}$ $\boldsymbol{z = xyx^{-1}y^{-1}}$

KEYWORDS: Lattice of Subgroup; Subgroup chains; Fuzzy Subgroup
MSC (2020): 20B30,20B35,20N25,20E15

INTRODUCTION

In Mathematics, group theory is one of the most important part of algebra. Group theory has an effective framework to analyze an object that appears in the symmetric form. It plays a vital role to classify the symmetries of molecules, atoms, regular polyhedral and crystal structures. This theory has become a standard and powerful tool to study universal genetic code and codon sequences behaviour. Group theory is the most important branch of Mathematics that has been broadly used in algebraic geometry, theoretical physics and cryptography.

The *Heisenberg* He_p is a 3-dimensional, simply connected, non- Abelian nilpotent group. For any odd prime p, Heisenberg group is the unique non-abelian group of order p^3 of exponent p. If one takes a, b, c in Z/pZ for an odd prime p, then one has the Heisenberg modulo p. It is a group of order p^3 with generators x,y and relations:

$\boldsymbol{x^p = y^p = z^p = 1, xz = zx, yz = zyz = xyx^{-1}y^{-1}}$

One of the most important problems in combinatorial group theory is to count the number of subgroup chains of a group. Many papers have treated various aspects of this problem in the last few years (Ogiugo et al.,2018, Adebisi et al., 2020, Leili et al.,2016) . The problem of counting chains of subgroups of a given group G has received attention by researchers classifying fuzzy subgroups of G under a certain type of equivalence relation (see Marius,2015, Ogiugo et al.,2017, Oh,2012) In this paper, we determined the number of chains of subgroups in the subgroup lattice of the Heisenberg Group using computational technique induced by isomorphism classes of subgroups of G.

PRELIMINARIES

Let G be a set and let $\mu: G \mapsto [0,1]$ be a fuzzy subset of G. If G be a group with a multiplicative binary operation and identity $\boldsymbol{e}$. Then μ is said to be a **Fuzzy Subgroup** of G if

(1) $\mu(xy) \geq \min\{\mu(x), \mu(y)\}$,
(2) $\mu(x^{-1}) \geq \mu(x)$ for all $x, y \in G$

And, since $(x^{-1})^{-1} = x$, we have that $\mu(x^{-1}) = \mu(x)$, for any $x \in$ G. Also, by this notation and definition, $\mu(e) = \sup \mu(G)$. For each $\alpha \in \mu$(G), the set $\mu\alpha := \{x \in G | \mu(x) \geq \alpha\}$ is called a **Level subset** of μ

Theorem 2.1 (Volf, 2004) : A fuzzy subset μ: G → [0, 1] of a group G is fuzzy subgroup if and only if all level subsets of μ are subgroups of G.

These level subsets allow us to characterize the fuzzy subgroups of G. This well-known theorem gives a link between the fuzzy subgroup lattice of G and the classical subgroup lattice of G.

Suppose that the group G is finite and let μ: G → [0, 1] be a fuzzy subgroup of G. Then μ (G) is a finite set, Put $\boldsymbol{\mu(G) = \{\alpha_1, \alpha_2, \ldots, \alpha_k\}}$ and assume that $\boldsymbol{\alpha_1 < \alpha_2 < \ldots < \alpha_k}$.

Then μ determines the following chain of subgroups of G which ends in

G: **{e}⊆ μGα₁ ⊂ μGα2 ⊂ ….⊂ μGαₖ = G**

Moreover, for any $x \in G$ and $i = \overline{1,k}$, we have

$$\mu(x) = \alpha_i \Leftrightarrow \alpha_i = max\{j|\ x \in \mu G\alpha_j\} \Leftrightarrow x \in \mu G\alpha_i \setminus \mu G\alpha_{1\text{-}k}$$

we set $\mu G\alpha_0 = 0$, then $\mu(e) = \alpha_i$

An adequate equivalence relation on the set of all fuzzy subgroups of the group must be defined to obtain a meaningful classification. Without any equivalence relation on fuzzy subgroups of group G, the number of fuzzy subgroups is infinite, even for the trivial group. We say that μ is equivalent to ν, written as $\mu \sim \nu$, if we have

$$\mu(x) > \mu(y) \Leftrightarrow \nu(x) > \nu(y), \forall x, y \in G,$$

and

$$\mu(x) = 0 \Leftrightarrow \nu(x) = 0, \forall x \in G.$$

Note that the condition $\mu(x) = 0$ holds if and only if $\nu(x) = 0$ simply says that the supports of μ and ν are equal and two fuzzy subgroups μ, ν of G are said to be distinct if $\mu \not\sim \nu$

This result shows that there exists a bijection between the equivalence classes of fuzzy subgroups of G and the set of chains of subgroups of G which end in G. So, the problem of counting all distinct fuzzy subgroups of G can translated into a combinatorial problem on the subgroup lattice of G that is finding the number of all chains of subgroups of G that terminate in G

Let G be a finite group and $\delta(G)$ be the number of chains of subgroups of G that terminate in G

$$\xi_1: G_1 \subset G_2 \subset \ldots \subset G_k = G \text{ with } G_1 \neq \{e\}$$
$$\xi_2: \{e\} \subset G_2 \subset \ldots \subset G_k = G$$

It is clear that the number of chains of types ξ_1 and ξ_2 are same and denoted by $\xi_1 = \xi_2$ if ξ_1 and ξ_2 contains same subgroups of G.

$$\delta(G) = \delta(\xi_1) + \delta(\xi_2)$$

RESULTS

Let $\delta(G)$ be the number of subgroup chains of group G that terminates in G. Then

$$\delta(G) = \sum_{distinct\ H\ \epsilon\ I\,so\,(G)} \delta(H) \times n(H) \ldots (\#)$$

Where

(i) $Iso(G)$ is the set of representatives of isomorphism classes of subgroups of G

(ii) $n(H)$ denotes the size of the isomorphism class with representative H

(iii) $\delta(H_e) = \delta(H_\alpha) = 1$, for which H_e is the trivial group of and H_α is the improper subgroup of G

In this work (#) was used to obtain the number of chains of subgroups of G that terminates in G and it was used in to count the number of distinct fuzzy subgroups of finite abelian group (Amit et al., 2016, Ogiugo & Amit, 2020)

Proposition 3.1:

Suppose that He_7 be the Cartesian product of group $(Z_7 \text{ x } Z_7) \ltimes Z_7$, then $\delta(He_7) =$ **260**

Proof :

Let G be He_7 has following set of representatives of isomorphism classes of sub- groups with their sizes: **[{e}, 1], [Z_7, 57], [Z_7 x Z_7, 8] and [(Z_7 x Z_7) ⋉Z_7, 1]**

$$\delta(Z_7 \text{ x } Z_7) \ltimes Z_7) = 1 + \delta(e) + 57 * \delta(Z_7) + 8 * \delta(Z_7 \text{ x } Z_7) = \mathbf{260}$$

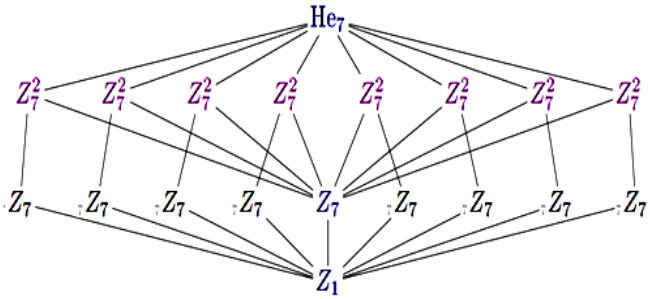

Obviously, this problem of counting all chains of subgroups of G depends entirely on the lattice of subgroups of G and not on the group itself.

Theorem 3.2:

Suppose that G be $(Z_p \text{ x } Z_p) \ltimes Z_p$, where p is any prime,

then

$$\delta(G) = \begin{cases} 32 & For\ P = 2 \\ 4p^2 + 8p + 8 & For\ p \geq 3 \end{cases}$$

For $p = 2, G$ is isomorphic to the Dihedral group of order 8 and when p is an odd prime, G is isomorphic to the Heisenberg Group

Proof. D_8 has the following set of representatives of isomorphism classes of subgroups with their sizes: [{e}, 1], [Z_2, 5], [Z_2 x Z_2, 2], [Z_4, 1] and [D_8, 1]

$$\delta(D_8) = 1 + \delta(e) + 5 * \delta(Z_2) + \delta(Z_4) + 2 * \delta(Z_2 \text{ x } Z_2) = \mathbf{32}$$

(Z_p x Z_p) $\ltimes$ Z_p has the following set of representatives of isomorphism classes of subgroups with their sizes:

He, Z_p $\{(p^2 + p + 1)\ times\}$, Z_p x Z_p $\{(p + 1)\ times\}$, and (Z_p x Z_p) $\ltimes$ Z_p

$\delta(Z_p \text{ x } Z_p) \ltimes Z_p)$
= 1+ $\delta(e)$+ $(p^2 + p + 1)$*$\delta(Z_p)$+(p+1)* $\delta(Z_p \text{ x } Z_p)$
= 2 + 2(p^2+p+1) + (p+1)(2p+4)
= 2 + 2p^2 + 2p + 2 + 2p^2 + 4p + 2p + 4
= 4p^2 + 8p + 8

CONCLUSION

This work also showed that a fuzzy subgroup is simply a chain of subgroups in the lattice of subgroups based on the natural equivalence relation. The study of the number of chains of subgroups in the lattice of subgroups for larger groups in classical group theory is very interesting. It will give rise to potential applications in solving the combinatorial problem of group testing for future pandemics within a larger population.

REFERENCES

Adebisi S. A., Ogiugo M. and EniOluwafe M. (2020). Computing the Number of Distinct Fuzzy Subgroups for the Nilpotent p-Group of D_{2n} x C_4 International J.Math. Combin. Vol.1,86-89.

Amit Sehgal, Sarita Sehgal, P. K. Sharma and Manjeet Jakhar(2016).Fuzzy subgroups of a finite abelian group Advances in Fuzzy Sets and Systems Vol. 21.4, 291-302.

Leili Kamali Ardekania, and Bijan Davvaz (2016). Classifying fuzzy (normal) subgroups of the group D_{2p} x Z_q and finite groups of order n < 20. Journal of Intelligent 4 Fuzzy Systems Vol. 33, 3615–3627.

J.-M. Oh(2012). The number of chains of subgroups of a finite cycle group. European Journal of Combinatorics, vol. 33 , no. 2, pp. 259-266.

M. Tărnăuceanu(2015). The number of chains of subgroups of a finite elementary abelian p-group. Politehn. Univ.Bucharest Sci. Bull. Ser. A Appl. Math. Phys. vol. 77 , pp.65-68.

Ogiugo M. and EniOluwafe M.(2017). Classifying a class of the fuzzy subgroups of the alternating group An. Imhotep Mathematical Proceedings Vol.4, 27- 33.

Ogiugo M. and EniOluwafe M.(2018). A new equivalence relation for the classification of fuzzy subgroups of symmetric group S_4 . Transactions of the Nigerian Association of Mathematical Physics Vol. 6 , pp. 168– 172.

Ogiugo M. and Amit Sehgal(2020). The number of chains of subgroups for certain alternating groups. Annals of Pure and Applied Mathematics, Vol. 22,No.1,65-70.

Volf, A. C.(2004). Counting fuzzy subgroups and chains of subgroups. Fuzzy Systems 4 Artificial Intelligence Vol. 10 , 191-200.